Advanced Technology of Switched Reluctance Machines in More Electric Aircraft: A Review

Lefei Ge, *Member, IEEE*, Nan Du, *Student Member, IEEE*, Jiahe Song, Jiaxin Zhang, Zizhen Fan, Dongpeng Zhang, and Shoujun Song, *Senior Member, IEEE*

***Abstract*—With the increasing focus on sustainable development and environmental preservation, the aviation industry has been exploring innovative solutions, such as more electric aircraft (MEA), to shape the future of air transportation. Among the various machines used in MEA, switched reluctance machines (SRMs) have gained significant attention due to their high reliability and excellent characteristics at high speeds. Delving into the forefront of SRM technologies, this article has summarized the advanced machine design, control strategies, fault diagnosis, and tolerant techniques, and the challenges of SRMs within the context of MEA. This article can provide resources for a deeper understanding of the latest developments in the technologies of SRM and help promote the application and development of SRM in the MEA field.**

***Index Terms*—Control, fault diagnosis, machine design, more electric aircraft (MEA), switched reluctance machine (SRM).**

Nomenclature

AFSRM	Axial-flux switched reluctance machine.
AVC	Active vibration cancellation.
CCC	Current chopping control.
DITC	Direct instantaneous torque control.
DOE	Design of experiment.
DRSRM	Double rotor switched reluctance machine.
DSSRM	Double stator switched reluctance machine.
DTC	Direct torque control.
EMF	Electromotive force.
FEA	Finite element analysis.
GA	Genetic algorithm.
GRSM	Global response surface method.
IM	Induction machine.
ITSC	Interturn short circuit.
MEA	More electric aircraft.
MPTC	Model predictive torque control.
MPT&FC	Model predictive torque and force control.
NN	Neural network.
NSGA-II	Nondominated sorting genetic algorithm II.
PDIV	Partial discharge inception voltage.
PM	Permanent magnet.
PMSM	Permanent magnet synchronous machine.
PWM	Pulsewidth modulation.
PSO	Particle swarm optimization.
RBF	Radial basis function.
RH	Relative humidity.
SMC	Sliding mode control.
SRG	Switched reluctance generator.
SRM	Switched reluctance machine.
SVM	Support vector machine.
TSF	Torque sharing function.
VC	Vector control.
WFSM	Wound field synchronous machine.

Received 24 April 2024; revised 25 July 2024; accepted 24 August 2024. Date of publication 30 August 2024; date of current version 12 December 2024. This work was supported in part by the National Natural Science Foundation of China under Grant 52107055 and Grant 52277067, in part by the Fundamental Research Funds for the Central Universities under Grant D5000230069, in part by the Aeronautical Science Foundation of China under Grant 20220040053001, in part by the Shaanxi Provincial Science Foundation for Distinguished Young Scholars under Grant 2023-JC-JQ44, in part by the Dreams Foundation of Jianghuai Advance Technology Center under Grant 2023-ZM01J001, and in part by research projects of AVIC Shaanxi Aero Electric Co., Ltd under Grant JSJSHT2312280030. Recommended for publication by Associate Editor Y. A.-R. I. Mohamed. *(Corresponding author: Shoujun Song.)*

Lefei Ge is with the School of Automation, Northwestern Polytechnical University, Xi'an 710072, China, and also with the Jianghuai Advance Technology Center, Hefei 230000, China (e-mail: lge@nwpu.edu.cn).

Nan Du, Jiahe Song, Jiaxin Zhang, Zizhen Fan, Dongpeng Zhang, and Shoujun Song are with the School of Automation, Northwestern Polytechnical University, Xi'an 710072, China (e-mail: dunan@mail.nwpu.edu.cn; sjhhhhh@mail.nwpu.edu.cn; zjxin@mail.nwpu.edu.cn; fanzizhen@mail.nwpu.edu.cn; zdp@mail.nwpu.edu.cn; sunnyway@nwpu.edu.cn).

Color versions of one or more figures in this article are available at https://doi.org/10.1109/TPEL.2024.3452171.

Digital Object Identifier 10.1109/TPEL.2024.3452171

I. Introduction

ELECTRIFICATION has become an important development direction in modern aviation technology and a key means to achieve sustainable and environmentally friendly aviation. To achieve the power density and reliability indicators required for aircraft applications, significant efforts have been made in the past few decades to improve the performance of MEA [1]. The concept of MEA was first introduced in the 1970s and has since received strong support from European and American countries. In the 1980s, the United States took the lead in implementing the "MEA Program." The arrival of the 21st century has witnessed the successful launch of several famous MEA models, including the Airbus A380 (the first commercial transport aircraft to use wired power technology), Boeing B787, Joint Strike Fighter F-35 (the first aircraft to have a fully electric wired flight control system) and the Chinese made C919 aircraft, heralding a new era in the field of aviation electrification [2], [3].

The electric machine technology is one of the core technologies of aircraft electrical systems and plays a crucial role in various systems, such as aircraft start/power generation, electromagnetic drive, and electric propulsion [4]. The aircraft requires

TABLE I
COMPARISON OF THE ELECTRICAL MACHINE PERFORMANCES IN AIRCRAFT

Source	Machine types	Voltage(V)	Power(kW)	Efficiency(%)	Power density(kW/kg)	Speed (r/min)	References
F-18	WFSM	115/200	40	78-80	/	27000	[7]
Honeywell	WFSM	600	1000	97	/	19000	[8]
Alexander C. Smith	IM	240	250	97	13.2	14000	[9]
UoN	PMSM	270	45	95	/	32000	[10]
NASA	PMSM	/	2600	98	11	3000	[11]
GE	SRM	270	250	90.8-93.1	5.3	22224	[12]
A.Chiba	SRM	650	60	89	2.4	13900	[13]
GE	SRM	105	30	89-93	3.89	50000	[14]

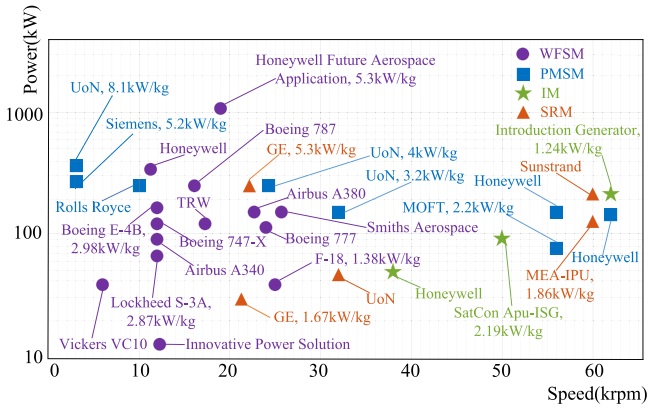

Fig. 1. Engines designed for aircraft systems [6].

high-precision control and faces strict conditions in terms of volume, propulsion, and stability, making the machine system more challenging than that in industrial and vehicle applications [5].

Currently, the field of MEA has focused on four types of machines: WFSM, IM, PMSM, and SRM. Fig. 1 shows the manufacturers and the performance characteristics of the engines designed for aircraft [6].

According to Fig. 1, it can be seen that PMSM has wide applicability under different working conditions. WFSM has a high power factor, good speed regulation performance, and high efficiency in the medium and low-speed fields. However, due to its mechanical structure and cooling limitations, it is unsuitable for high-speed fields, limiting its application in MEA. Specifically, SRM and IM exhibit their advantages in the higher speed range.

SRM employs multiphase design and power division techniques to ensure safe operation during faults, contributing to their strong fault tolerance and robustness [15]. The solid rotor structure of SRM, which is composed of laminated silicon steel sheets, endows it with the ability to withstand high temperatures up to 400 °C. In contrast, PMSM and IM are more susceptible to impact in high-temperature aviation environments. The PMSM is limited by the thermal characteristics of the PM, with maximum operating temperatures mostly below 200 °C, while IM can handle temperatures up to 250 °C [16], [17]. Furthermore, SRM exhibits superior electromagnetic reliability and is particularly well-suited for high-speed applications [18].

Table I shows the machine parameters in development and application for aircraft [4], [19]. Overall, machines in MEA are developing toward higher power density and have certain requirements for efficiency.

Considering factors, such as power density, speed, and temperature, the SRM exhibits unique advantages in multiphase machine performance. However, in MEA applications, SRM faces increasing demands and challenges related to achieving higher power density, efficiency, stability, and environmental adaptability within limited space [20]. By analyzing the advantages and limitations of the SRM, combined with the requirements of MEA applications, practical solutions, and optimization strategies can be provided for the SRM systems.

In this article, we provide a comprehensive overview of SRM technology, covering machine design, control strategies, fault diagnosis, and tolerant control. By summarizing existing research, this article has evaluated the practical challenges and response strategies of existing research methods for SRM in MEA applications. In addition, it also evaluated practical application cases of SRM, explored its challenges in environmental adaptability, weight and volume limitations, and electromagnetic interference, and identified future research needs and gaps to advance SRM technology in the MEA field.

The rest of this article is organized as follows. Section II analyzes the current demand for SRM in aviation and provides evaluation methods corresponding to the indicators. Section III focuses on the design of the SRM, including parameter optimization techniques and novel machine structures. Section IV investigates the latest research on control methods and evaluates the gap between existing studies and the demand for high-performance aviation. Following that, Section V introduces the fault diagnosis and the fault tolerance techniques for SRM. In Section VI, practical applications of the SRM in aircraft are discussed, along with the existing challenges and future trends. Finally, Section VII concludes this article.

II. REQUIREMENT ANALYSIS OF SRM FOR MEA

The integration of the SRM, especially on advanced military aircraft, such as the F-35, highlights the potential for more straightforward, reliable, and fault-tolerant power solutions. However, there are still many issues with the application of SRM, the most significant of which are the lower efficiency compared to PMSM and its inherent torque ripple problem. Conducting a

TABLE II
POWER DENSITY REQUIREMENT OF ELECTRIC MACHINES FOR VARIOUS AIRCRAFT TYPES AND ARCHITECTURES [16]

Aircraft types	Aircraft architecture	Power density(kW/kg)
General aviation and commuter	Parallel hybrid	> 3.0
	Turbo-electric	> 6.5
Regional and single aisle	Parallel hybrid	> 3.0
	Turbo-electric	> 6.5
Twin aisle	Turbo-electric	> 10.0

requirement analysis of SRM in response to the aircraft can help to carry out targeted optimization and analyze the shortcomings of current strategies.

A. Analysis of Existing Circumstances

Before World War II, the design speed of early dc aircraft generators was between 3000 and 10000 r/min, with a power density not exceeding 0.4 kW/kg and a maximum power generation of 22.5 kW. At the same time, British V-bombers had already applied ac generators that could generate 50 kW of power [15].

The speed of modern dc generators can reach 13 000 r/min, but the power density is still relatively low, rarely exceeding 1 kW/kg [15]. The implementation of the SRM in aviation was first observed during the 1980s, initially in military aircraft. In 1995, a high-speed SRM was designed for aircraft engines [21], which can reach a speed of 52 000 r/min, a power density of 3.89 kW/kg, and can withstand a temperature range of -50 to 125 °C. However, its efficiency can only reach 80%, limiting its wider range of applications. The deployment of SRM is particularly prominent on Lockheed Martin's F-22, which was officially put into use in 2005, and the F-35 fighter jet launched in 2015, both of which use 270 V dc-power supply and achieve power levels of 70 and 80 kW [19]. A 32 000 r/min high-speed SRM developed in 2017 also demonstrated the shortcomings of SRM in efficiency, which can only reach 82% [22], [23]. A collaboration between the USAF, GE, Sundstrand Aerospace, and the University of Kentucky resulted in an aerospace SRM with a 250 kW power output at 22224 r/min [12], [24]. It has achieved a high power density of 5.3 kW/kg and an efficiency of up to 90.8%–93.1%, demonstrating the enormous potential of SRM [12].

Significant progress has been achieved in improving the performances of SRMs for MEA. However, further enhancements are still possible. Future development will focus on improving power density and efficiency, expanding the operating temperature range, reducing volume and weight, and enhancing reliability and durability to meet the growing demand for aviation.

B. Machine Design Requirements

The power density requirements for electric machines in MEA depend on the aircraft type and electrification architecture. As aircraft size and complexity increase, so does the demand for power density in machines. Table II lists the power density requirements for various aircraft types and structures, which must be the primary consideration in the machine design process.

Moreover, in the process of machine design, it is necessary to improve the efficiency as much as possible to ensure the efficient operation of the aircraft. The simplicity of the structure is also a factor that must be considered, which is crucial for reducing failure rates and costs. In addition, excellent thermal management is required for stable operation in high-temperature environments, especially above 200 °C.

C. Machine Control Requirements

The SRM must maintain efficient operation under different working conditions, but the current efficiency level of SRM is usually only above 80%. To achieve the widespread application of MEA, it is necessary to optimize the SRM control method to achieve an efficiency of over 90%, which can help extend endurance and reduce energy consumption.

Torque ripple can cause vibration and noise, affecting the comfort and equipment lifespan. To reduce the vibration and noise, optimization algorithms should be used to minimize the torque ripple while ensuring stable output of machine torque, and to control the vibration of the machine system at the lowest level possible.

The equation for evaluating the torque ripple used in this article is

$$T_{\text{rip}} = \frac{T_{\max} - T_{\min}}{T_{\text{avg}}} \times 100\% \tag{1}$$

where $T_{\max}$ and $T_{\min}$ are the maximum and minimum values of torque in steady state, and T_{avg} is the average value of the torque, which is considered as the output torque, given as

$$T_{\text{avg}} = \frac{1}{t_2 - t_1} \int_{t_1}^{t_2} T(t)dt \tag{2}$$

where t_1 and t_2 are the start and end of a rotor position period.

D. Fault Diagnosis and Tolerant Requirements

For fault diagnosis, MEA applications need to ensure detection accuracy and speed, as well as high coverage of fault identification. In certain fault situations, the system should be able to continue operating with at least 70% power output to ensure flight safety. After implementing fault-tolerant control, the system should remain stable without obvious oscillation or loss of control. In different fault situations, the time from detecting the fault to executing fault-tolerant measures should meet the response time requirements.

In summary, the current situation indicates that modern SRM has made significant progress in aircraft. This section analyzes the requirements of MEA for SRMs, covering machine design, control, fault diagnosis, and tolerant requirements. Through the discussion of these aspects, a foundation has been laid for further exploration of the problems and solutions in various current technologies.

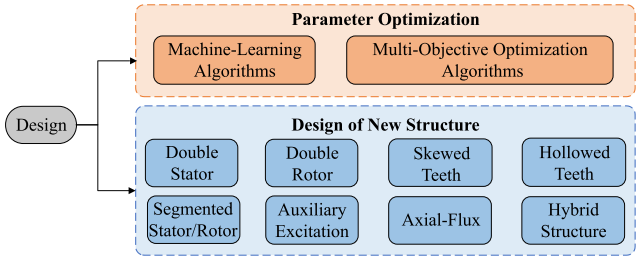

Fig. 2. Classification of machine design.

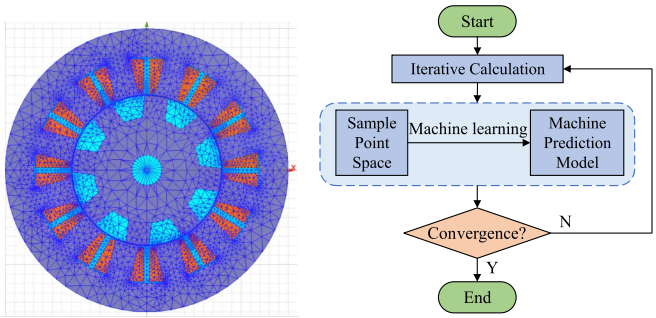

Fig. 3. Optimization process of machine learning. (a) Discretization of SRM. (b) Optimization process.

III. Design

The machine design is critical to ensuring the system performance and aviation safety. This section has summarized the recent research on the design of SRMs, aiming to evaluate the effectiveness of current studies in improving the performance of machines and explore how to improve power density and efficiency by developing reasonable and effective new optimization algorithms and topology designs. The content included in this section is shown in Fig. 2.

A. Parameter Optimization Methods

The structural parameters of the SRM can significantly affect its performance. Through numerical simulation and algorithm optimization, the number of iterations in the design process can be effectively reduced, thereby reducing design costs and time. Currently, machine learning and multiobjective optimization are two mainstream parameter optimization strategies.

1) Machine Learning Algorithms: Machine learning algorithms can predict the impact of different structural parameters on SRM performance through a large amount of training data, which can significantly reduce the number of actual tests and save time and resources.

Fig. 3 shows the process of optimizing the machine parameters through machine learning fitting models. First, the machine structure is discretized through FEA to obtain a dataset consisting of machine optimization parameters and optimization objectives [25], [26], as shown in Fig. 3(a). Then, a dataset is used as input and trained through a machine learning model to obtain a fitting model for optimization parameters and optimization objectives, as shown in Fig. 3(b).

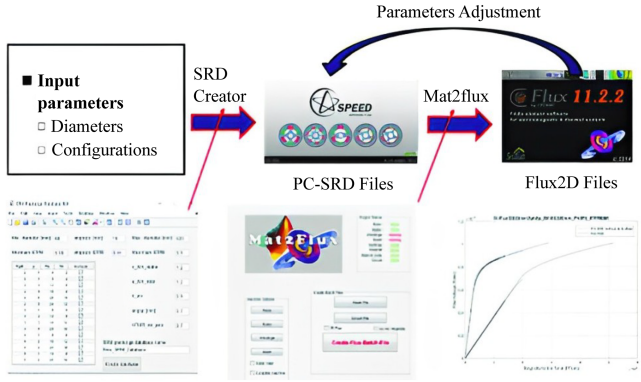

Fig. 4. Generation process of SRM database in [27].

In [27], a data-based design method for SRM has been proposed, as shown in Fig. 4. This method has established a machine loss model by calling SRM databases with different structures, reducing the complex iterative operations of machine learning. The machine designed by this method can achieve a power of 200 kW at a speed of 3000 r/min, with a high torque density of 11.49 N · m/kg and a power density of 2.86 kW/kg. However, at an average torque of 804.5 N · m, its torque ripple is 44%, which still needs to be optimized for aviation applications.

Machine learning algorithms have been widely applied in SRM modeling. However, they may produce sub optimal results in prediction accuracy and error when trained without intelligent optimization algorithms. Different intelligent optimization methods can be combined in the SRM optimization application of MEA to make up for its shortcoming. For example, PSO can be used to optimize SVM models [28], while differential evolution algorithms can be used to optimize extreme learning machines [29]. In the future, with improved computing resources and algorithms, integrating multiple optimization methods will enhance the performance and efficiency of SRM.

2) Multiobjective Optimization Algorithms: Multiobjective optimization algorithms combine optimization algorithms with multiphysical field electromagnetic calculations through interface programs. The parameters are generated through an optimization algorithm and then transferred to the FEA software for analysis through a script file. Once the analysis is completed, the results are transferred back to the algorithm for selection, creating a closed-loop optimization process. This process has been shown in Fig. 5.

In [30], a model fitting method using surrogate models and global optimization methods was proposed, as shown in Fig. 6. This method was based on the DOE, utilizing two nonlinear surrogate models [NN and RBF], as well as three optimization algorithms (GA, GRSM, and PSO). This global optimization model has more robust adaptability, effectively overcoming the limitations of a single machine learning method and improving the generalization ability of the model.

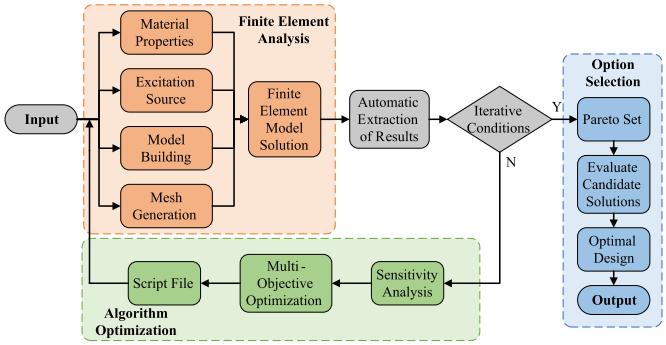

Fig. 5. Process of multiobjective optimization.

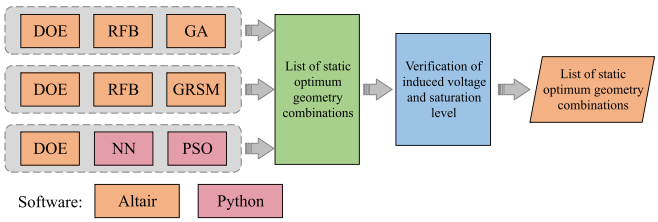

Fig. 6. Global optimization method in [30].

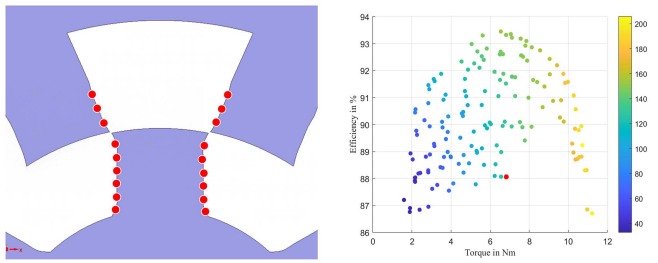

Fig. 7. Finite element model optimization and Pareto set. (a) Teeth profile adjusting. (b) Real optimized Pareto set.

By using the multiobjective differential evolution algorithm, multiobjective PSO, and multiobjective GA optimization algorithm separately for optimization of parameters, the efficiency, average torque, and torque ripple of the SRM can been effectively improved [31].

In [32] and [33], multiobjective optimization design methods have been adopted, combining FEA and NSGA-II. Through multiple iterations, these algorithms can generate a realistic Pareto set for balancing the best solution between different design objectives. By using these methods, combined with the modified teeth profile parameters, the finite element model of the SRM can be refined, as shown in Fig. 7.

Abunike et al. [34] demonstrated the effectiveness of the NSGA-II algorithm in optimizing the objective function, resulting in a 15% increase in average torque and achieved an output efficiency of 96.2%. Meanwhile, the optimization time was reduced from 65 to 10 min. In another research, Hua et al. [32] used the NSGA-II algorithm to increase the average torque of a machine by 28.92% and decrease the torque ripple by 65.91%, achieving a final torque ripple of about 10%.

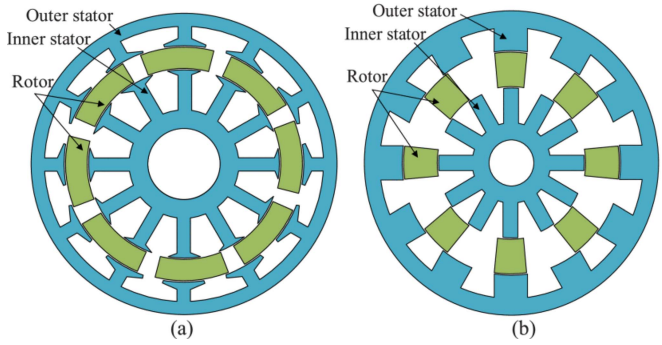

Fig. 8. Two types of DSSRM in [37].

Local optimization, also known as preference optimization, integrates the preference information of decision-makers into multiobjective optimization algorithms to enhance the ability of the algorithm to generate individuals within the preference domain. In [35], a multiobjective preference optimization method based on NSGA-II is proposed. However, this algorithm has a torque ripple of around 40% and an efficiency of around 80%, which needs further exploration for its application in MEA.

In summary, multiobjective optimization algorithms can achieve more precise and efficient optimization by effectively quantifying the relative importance and difficulty of each objective. However, further research and improvement are still needed on issues, such as torque ripple and efficiency. Future research directions should focus on improving optimization algorithms, conducting practical application testing, and exploring multiobjective tradeoff strategies.

B. *Design of new Structures*

In applications with high-temperature in aerospace, the design of the SRM faces particular challenges [36]. The changes in geometric dimensions under high temperatures may reduce the performance of SRMs, affecting their power output and efficiency. Research on improving SRM performance indicators through new structural designs mainly focuses on stator and rotor structures, as well as excitation modes.

1) Double-Stator SRM: The typical DSSRMs are shown in Fig. 8 [37]. The use of a dual stator structure increases the available winding area and has a high torque density. This structure can significantly reduce the volume and weight of the mechanical system and improve the accuracy and dynamic performance of the system in limited space.

A DSSRM with opposite excitation between the inner and outer stators is an efficient structure. This design lowers inductance values and reduces current demand, resulting in lower loss under various conditions and superior power conversion ratios. In [27] and [38], power densities of 2.86 and 1.83 kW/kg were achieved.

2) Double-Rotor SRM: In the design of a DRSRM, two independently configured rotors can be designed to meet two different torque-speed characteristics [39]. Compared with traditional

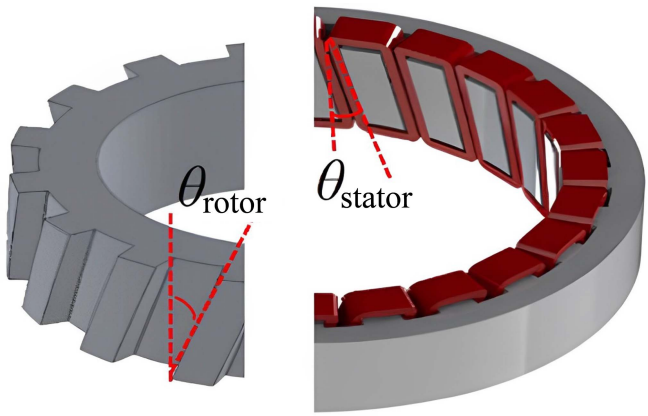

Fig. 9. Teeth-skewed SRM in [42].

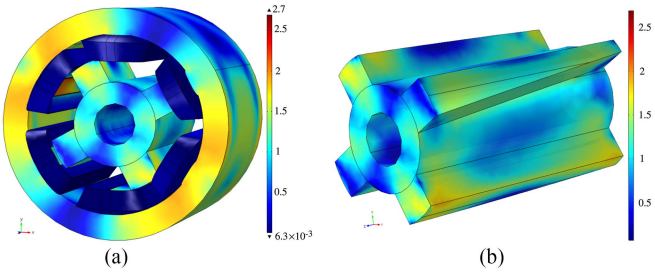

Fig. 10. Skewed rotor SRM in [43]. (a) Overall structure of the SRM. (b) The rotor with skewed poles.

SRM, the DRSRM proposed in [40] increases the average torque by 23%. The torque improvement will provide an effective solution for aircraft with high load conditions, but its efficiency still needs to be considered.

3) Teeth-Skewed SRM: By deflecting the teeth of the machine from the vertical direction to a specific angle, the teeth-skewed design changes the magnetic field distribution within the SRM [41]. A design with skewed teeth is shown in Fig. 9 [42]. By expanding the air gap of the rotor slot, the inductance generated when the rotor and stator are not completely aligned can be reduced, which helps to maintain high torque output at high speeds and reduce torque ripple. By using skewed teeth, torque ripple can be reduced by 43.09%.

As shown in Fig. 10, in addition to the parallel skewed teeth, a unique skewed rotor pole shape was also proposed in [43], which reduces the torque ripple of traditional SRM from 32.25% to 20.21%. The major problem with teeth-skewed SRM currently also lies in its efficiency, as the efficiency of only 60% in [41] is clearly too low.

4) Teeth-Hollowed SRM: Guidkaya et al. [44] proposed a novel rotor-shaped 6/2 SRM with a hollow teeth structure, which has increased the acceleration zone of the SRM. In [45], the design of circular and elliptical voids of SRM was studied, as shown in Fig. 11.

Setting hollow structures on the SRM can increase the reluctance around the poles, thereby reducing radial forces and achieving vibration suppression. However, this will also reduce

Fig. 11. Teeth hollowed SRM in [45].

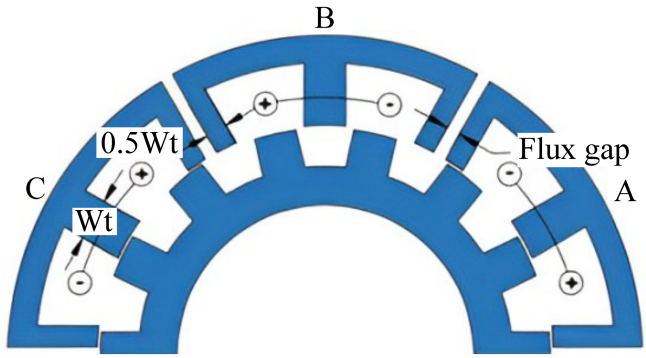

Fig. 12. Segmented-stator SRM in [46].

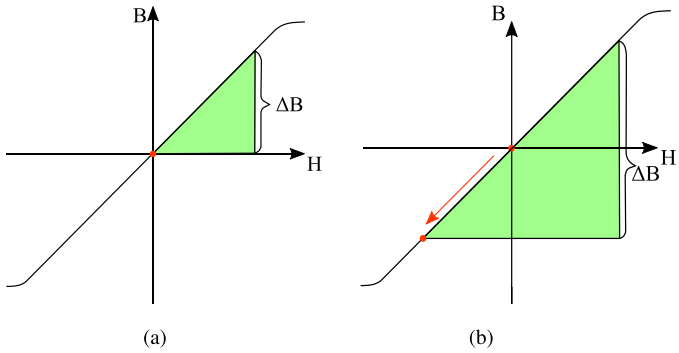

Fig. 13. B-H curve and working area of the SRM [55]. (a) Traditional SRM. (b) SRM with PM assisted.

the tangential force and affect the average torque, which is a consideration in the design process.

5) Segmented-Stator/Rotor SRM: The segmented-SRM features multiple independent iron cores in the stator or rotor, embedded in nonmagnetic support components, as shown in Fig. 12 [46]. This design aims to achieve shorter magnetic circuits to reduce iron loss and torque ripple. Mehta et al. [47] has proposed a segmented-rotor SRM that has reduced torque ripple to 3.6%. Although its power is only designed to be 120W, the extremely low torque ripple proves its potential for development. In addition, a segmented-rotor SRM proposed in [48] can generate higher output torque and reduce the number of turns per phase by 20%, but the efficiency is only 80.68%.

6) Auxiliary Excitation SRM: In the SRM, the operating range is usually limited to the first quadrant of the B-H curve, as shown in Fig. 13(a). By introducing magnetic materials to

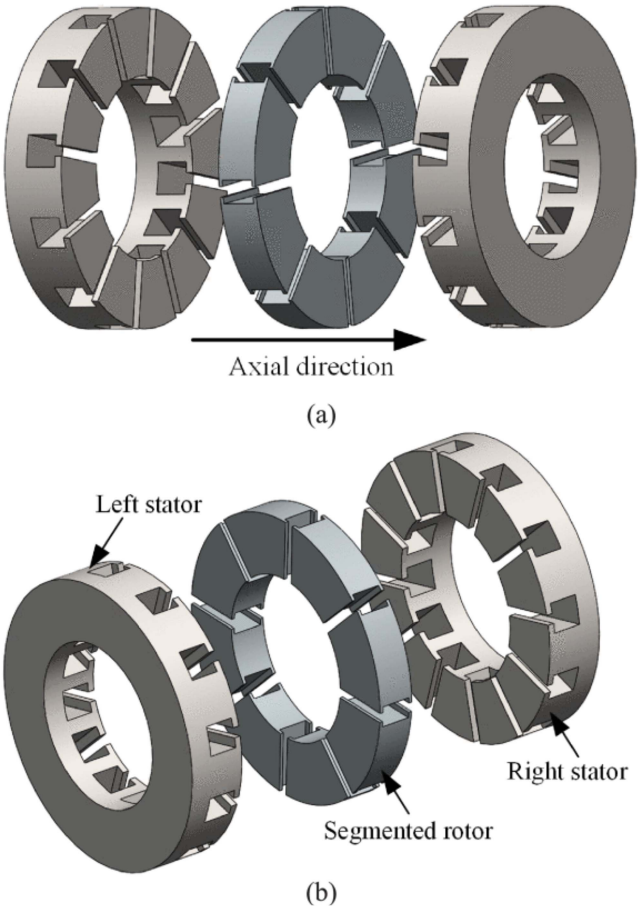

Fig. 14. AFSRM in [54].

reverse bias the stator core, the characteristics of the magnetic circuit can be changed, allowing the machine to be effectively controlled and utilized in the third quadrant [55], as shown in Fig. 13(b). This method of expanding the working range improves the performance of the SRM, especially under high loads or fast dynamic response requirements, providing greater torque output [56].

The team of Farahani [49] has demonstrated that PM-assisted structures can achieve higher torque and power. In the design of [57], PM is used between the end teeth of adjacent modules in SRM. Under the same excitation current, the average torque has been increased by 67.8%.

7) Axial-Flux SRM (AFSRM): The AFSRM transfers flux along the axis direction of the rotor and stator, as shown in Fig. 14. Recent studies have found that axial-flux structures can provide higher power density, efficiency, and faster response speed [54]. In [50], grain-oriented electrical steel was applied to the AFSRM to improve its torque characteristics, resulting in a maximum torque increase of 20.5% and achieving the efficiency of 90.1%..

8) Hybrid Structure SRM: Various combinations of novel SRM structures have been proposed to address the different impacts of different structures on SRM characteristics. Ghaffarpour has proposed a segmented double rotor PM SRM, which can reduce torque ripple to 10.9% [51]. Kondelaji and Mirsalim [52] have proposed a segmented rotor double stator SRM, resulting in less iron consumption, shorter flux linkage paths, and lower losses. The authors in [53], [57], and [58] have proposed SRMs that combine segmented stator and PM-assisted excitation, in which the PM was used to increase torque without limiting winding area or reducing machine robustness. In [59], a dual stator hybrid excitation modular variable reluctance machine was proposed, with good static torque characteristics and dynamic performance. In [60], an axial-flux double rotor segmented SRM was proposed to minimize unwanted torque ripple. By combining the optimization of opening and closing angles, the torque ripple coefficient has been reduced by about 73%.

According to the survey, the performance comparison of different machines is presented in Table III. By comparing the performance of output power, torque ripple, and efficiency, the adaptability and limitations of the SRM new structure for MEA applications can be analyzed as follows.

1) Output power: The power of DSSRM and teeth-skewed SRM has been designed to meet the high-power demands of up to 100 kW. However, most newly developed configurations currently yield less than 1 kW. Further research and improvement of power output methodologies are needed, such as the optimization of magnetic circuit design and utilization of high-performance materials.
2) Torque ripple: Some new structures, such as segmented SRM and PM-DRSRM, perform well in torque ripple suppression, but their testing environments are limited to low-power machines. Conducting torque ripple performance verification at higher power and torque can provide an effective solution for improving the stability of SRM used in MEA.
3) Efficiency: Except for AF-PMSRM, which can achieve an efficiency of 90%, the efficiency of most other new structures is below 85%, indicating significant room for improvement. Further research is needed on methods to improve efficiency and reduce energy loss, such as improving cooling systems and applying efficient control algorithms. In addition, lower power output is also one of the factors leading to low efficiency. It is necessary to test different structures under higher power output conditions to verify their efficiency performance under high loads.

In summary, the new SRM structures still require extensive research on power and efficiency improvement while maintaining and further optimizing torque ripple suppression technology to meet the application requirements of MEA.

IV. Control

Due to the inherent nonlinear characteristics of the SRM, its control is relatively more difficult [61], [62]. The traditional CCC method has been proven to apply to aircraft [14], [21], [22], [23], [63], exhibiting good performance at high power levels and high voltages. However, under the traditional CCC method, the nonlinear effects of the SRM will be amplified, which may lead to decreased control accuracy and poorer dynamic performance. At the same time, the current undergoes significant changes

TABLE III
PERFORMANCE COMPARISON OF SRM MACHINES WITH DIFFERENT STRUCTURES

Machine Type	Pole number	Voltage(V)	Power(kW)	Speed(r/min)	Torque ripple(%)	Efficiency(%)	Reference
DSSRM	16/12/16	750	200	3000	44	/	[27]
DSSRM	16/18/16	48	1.5	600	29.7	/	[37]
DSSRM	12/8/12	300	100	3000	20	83.34	[38]
DRSRM	8/6/6/4	300	/	2000	/	87	[39]
Teeth-skewed SRM	24/16	600	100	4250	/	/	[42]
Teeth-skewed SRM	6/4	/	/	3000	20.21	/	[43]
Segmented SRM	12/8	12	0.12	1800	3.6	/	[47]
Segmented SRM	12/8	/	0.5	2800	/	80.68	[48]
PM-SRM	12/10	120	0.3	600	/	73.2	[49]
AF-PMSRM	/	150	2	600	/	90.1	[50]
PM-DRSRM	/	/	0.5	1000	10.9	83.6	[51]
Segmented-DSSRM	12/14/12	50	0.32	800	64.8	80.2	[52]
Segmented-PMSRM	12/10	210	0.6	2000	57.2	84.3	[53]
AF-DSSRM	12/8/12	96	1.5	1000	30.7	/	[54]

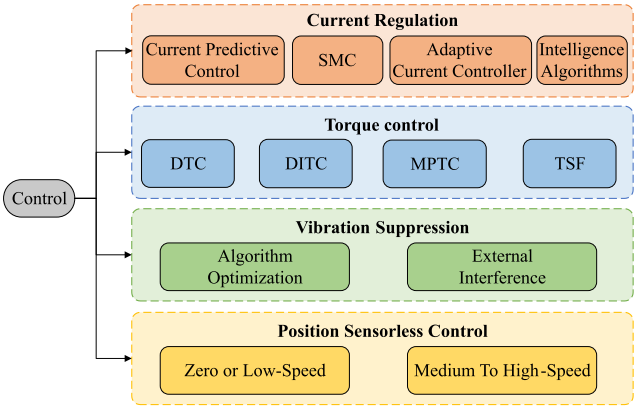

Fig. 15. Classifications of the control method.

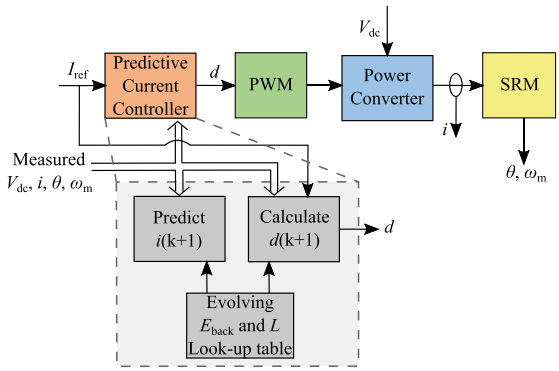

Fig. 16. Current predictive control method in [66].

quickly, which can easily generate high-frequency noise and vibration [64].

Researchers have been exploring and developing various advanced control strategies to improve the performance, efficiency, and stability of the SRM. As Fig. 15 shows, this section focuses on the latest solutions for advanced SRM control methods, including current regulation, torque control, vibration suppression, and position sensorless technology [65].

A. Current Regulation

Accurate tracking of the reference current waveform is crucial for obtaining the required average torque and minimizing the torque ripple and losses in SRM. Most new current regulation methods have focused on improving the accuracy of current control.

1) Current Predictive Control: Traditional current prediction is based on lookup tables. In [66], a lookup table for incremental inductance and back EMF coefficient was established, and based on the lookup table, a constant current injection scheme for PWM constant frequency current predictive control was proposed, as shown in Fig. 16.

Although a lookup table is an effective solution, changes in the operating state may result in actual conditions not matching the original model used in the design, which may affect the accuracy and effectiveness of lookup tables. A current prediction control method that eliminates lookup tables is of great significance for eliminating the dependence of control schemes on models [67], [68].

In current research, current predictive control has been applied to high-performance SRM control schemes, achieving torque ripple as low as 15.63% [69], [70].

2) Sliding Mode Control (SMC): The SMC is a commonly used control strategy for achieving high-performance control of SRM systems. The core idea is to guide the system state to the sliding surface by designing appropriate sliding mode surfaces and SMC laws, thereby achieving control of the dynamic response, as shown in Fig. 17.

In [72], a digital sliding mode pulsewidth mode current control method is proposed, which eliminates the need for identifying phase inductance or flux linkage. In [73], a direct second-order SMC method is proposed to minimize the current distortion and torque ripple of SRM. The successful application

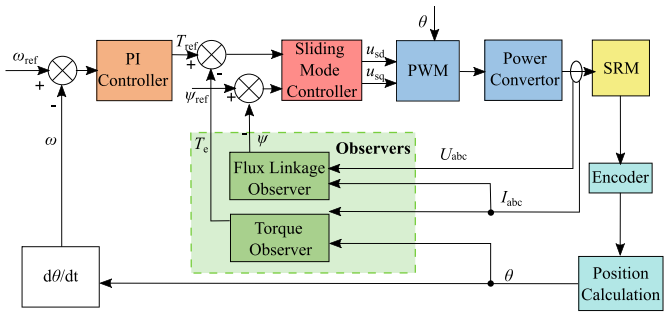

Fig. 17. Block diagram of SMC.

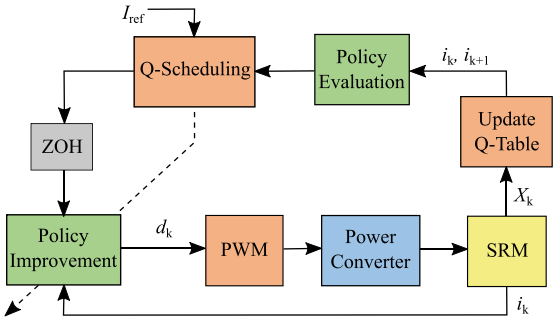

Fig. 19. Block diagram of Q-learning method in [78].

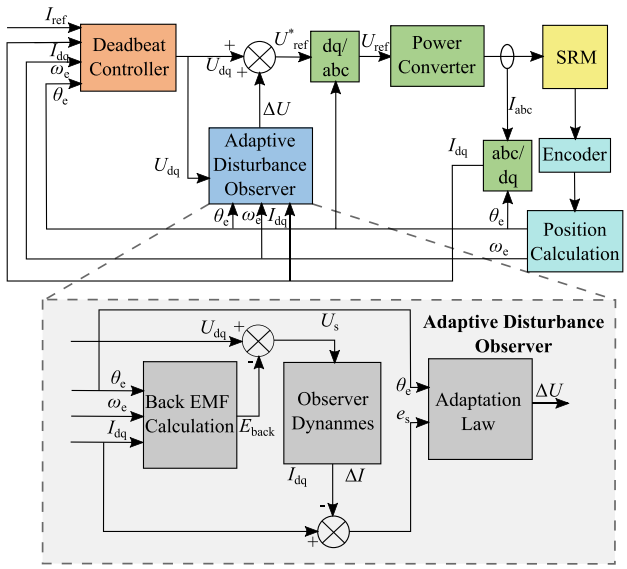

Fig. 18. Block diagram of adaptive current control [75].

of SMC method in an SRM with 60 kW and 15 N · m proves its applicability for high power and torque [71]. The effective suppression effect of SMC on torque ripple has great research significance for maintaining the stability of MEA.

3) Adaptive Current Control: The adaptive current control can adjust parameters in real time based on the dynamic characteristics of the system. It can maintain the stability of the system in the event of changes in system parameters or external disturbances, as shown in Fig. 18.

An adaptive flux linkage observer based on Lyapunov has been proposed for the severe dependence on the accurate flux linkage model [74]. In [75], considering the neglect of system uncertainty caused by magnetic saturation during the modeling process, a superficial adaptive disturbance observer based on the steepest descent method was embedded in the deadbeat controller, thereby improving the stability of the system.

Although the dependence on the model can be reduced, the accuracy of adaptive current control must be compensated for through algorithm improvement. Excessive torque ripple is one of the difficulties in its practical application in research.

4) Intelligence Algorithms: Intelligent algorithms can effectively manage nonlinear characteristics to achieve precise system control. Alharkan et al. [78] proposed a novel Q-learning scheduling method for the current control of SRM, as shown in Fig. 19. This method, based on the reference current signal, successfully tracked the reference current trajectory without requiring model parameter information. In [76], the application of GA in SRM commutation angle optimization was developed, and the proposed method reduced torque ripple by more than 50%. In [77], the preprocessing method verified that a back propagation NN model based on the Levenberg Marquardt algorithm resulted in higher control accuracy.

Table IV lists the key indicators of various methods used in this research. The applicability and limitations of different current regulation methods for MEA applications can be analyzed by comparing the indicators.

For MEA applications, current predictive control and SMC methods are more suitable due to their higher power capability and relatively manageable torque ripple. SMC is particularly promising because of its low torque ripple (10.06% to 13.2%), although it requires careful implementation. Although adaptive current control and intelligent algorithms are innovative, they face significant challenges in terms of torque ripple (up to 95.41% and 60%) and output power, which will limit their use in critical MEA systems.

B. Torque Control

The torque control of the SRM dynamically adjusts the torque output of the machine based on actual load requirements. By optimizing the torque output, the system can achieve optimal performance under different working conditions, improving efficiency and performance. The current hotspots in torque control research include DTC, DITC, MPTC, TSF.

1) Direct Torque Control: DTC is a widely used method for the control of SRM, which can be applied to reduce their inherent output torque ripple. The basic DTC method diagram has been shown in Fig. 20. The traditional DTC method may lead to negative torque in certain situations, thereby reducing the torque–current ratio of the SRM. By adjusting the turn-off angle in real-time, negative torque can be avoided [80]. Although the DTC method can improve system performance, it is sensitive to changes in machine parameters and requires precise parameter adjustment and calibration in practical applications.

TABLE IV
PERFORMANCE COMPARISON OF DIFFERENT CURRENT REGULATION METHODS FOR SRM

Method	Machine types	Power(kW)	Speed(r/min)	Torque(N·m)	Torque ripple(%)	References
Current Predictive Control	6/4 SRM	60	1000	10	21	[69]
	8/6 SRM	4	1500	24	15.63	[70]
	8/6 SRM	2.2	3000	8	24.03	[67]
SMC	6/4 SRM	60	800	15	13.2	[73]
	12/8 SRM	1.2	2500	1	/	[71]
	8/6 SRM	1.2	1500	25	10.06	[72]
Adaptive Current Control	8/6 SRM	5.1	6000	3	/	[74]
	12/8 SRM	1.5	1500	9.5	95.41	[75]
Intelligence Algorithms	8/6 SRM	2	600	0.7	60	[76]
	12/8 SRM	1.5	1500	9	/	[77]

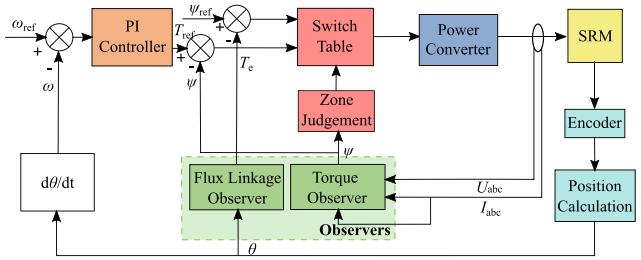

Fig. 20. Block diagram of DTC.

2) Direct Instantaneous Torque Control: DITC tends to control torque under instantaneous conditions. In [81], based on the DITC method, the efficiency and torque ripple coefficient have been combined to form an objective function, and GA was used to optimize the commutation zone online. In addition, DITC scheme based on adaptive dynamic commutation strategy can effectively reduce torque ripple and improve system efficiency [82].

DITC has a fast response speed and can achieve fast torque adjustment, making it suitable for applications that require high dynamic performance. However, during low-speed operation, it will generate significant torque ripple, which is still a problem that needs to be studied.

3) Model Predictive Torque Control: MPTC can accurately predict the future state based on the machine model and achieve high-precision torque control, improving the control accuracy and stability. Ge has proposed an MPTC to suppress torque and power supply current ripple, as shown in Fig. 21 [83], [84]. By predicting torque and power current ripple under different switching states and constructing a cost function, mechanical vibration can be reduced.

In addition, the new MPTC method includes combining with PWM control signals [85], [87], constructing fourth-order Fourier series torque and current models [91], and so on. The MPTC method requires highly accurate machine models for solving complex and computationally intensive optimization problems in real time. Practical application needs to consider computational accuracy and system computation time, which are gradually being addressed with the continuous upgrading of processors.

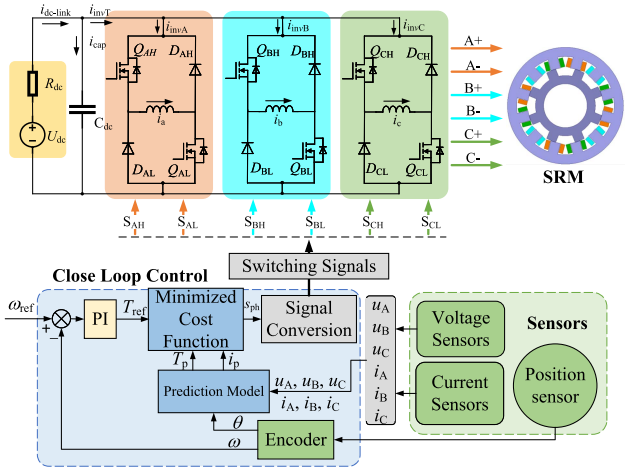

Fig. 21. Block diagram of MPTC in [83].

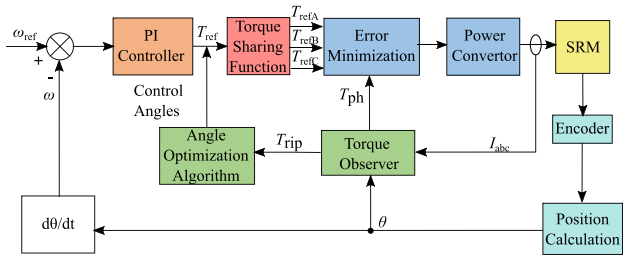

Fig. 22. Block diagram of TSF control [52].

4) Torque Sharing Function: The TSF method allocates the total torque to each phase based on the function, ensuring that the total torque of each phase at any time remains stable. The control principle is shown in Fig. 22 [88].

In [88], an offline TSF for torque ripple suppression in SRM was introduced, using the static flux linkage characteristics to determine the optimal current distribution. Xia et al. [89] considered the rise and fall of phase current and combined the conduction angle and turn-off angle in current reference

TABLE V
PERFORMANCE COMPARISON OF DIFFERENT TORQUE CONTROL METHODS FOR SRM

Method	Machine types	Power(kW)	Speed(r/min)	Torque(N·m)	Torque ripple(%)	References
DTC	8/6 SRM	2.2	1500	3	22.4	[79]
	12/8 SRM	/	5000	0.6	16.67	[80]
DITC	12/8 SRM	/	1500	2.5	47.21	[81]
	12/8 SRM	0.75	1500	2	60	[82]
MPTC	12/8 SRM	1	1200	2	32.97	[83], [84]
	12/8 SRM	1	1000	4	32.71	[85]
	12/8 SRM	1	1300	1	31.25	[86]
	12/8 SRM	1	1500	4	62.27	[87]
TSF	8/6 SRM	5.2	6000	4	37.5	[88]
	12/8 SRM	2	1000	20	56.65	[89]
	12/8 SRM	1	1000	2	31.58	[90]

generation, achieving more comprehensive optimization during commutation zone. In [90], a new TSF based on flux linkage derivation was introduced, which thoroughly considered the actual torque generation ability of SRM at different rotor positions.

In addition, the TSF method has been combined with online current contour generation technology [92] and MPTC [93], [94], which can achieve better performance and control accuracy through the new TSF.

The TSF method can achieve precise torque control by optimizing current distribution to minimize torque ripple and improve system control accuracy. However, implementing the TSF method may require more complex control strategies and algorithms.

By summarizing the torque control methods in this paper in Table V and comparing the comprehensive requirements of MEA, the current status of SRM research can be analyzed. DTC can achieve high speed and low torque ripple (16.67%), suitable for high-speed operating systems. DITC has relatively high torque ripple, limiting its use in applications requiring stable output. The torque ripple of MPTC varies greatly, and further optimization is needed to improve its stability in practical applications. TSF has a wide range of torque applications, making it suitable for high-load applications.

Currently, some new torque control methods are not suitable for high-power machines, posing a challenge for MEA applications. Future research needs to focus on improving torque control precision and validating machines at higher power levels. Efficiency indicators are not prominent in current research, so targeted development and validation of algorithm efficiency is essential for high-performing MEA.

C. Vibration Suppression

When applying the SRM to aircraft, the vibration can cause friction and energy loss of aircraft mechanical components and even damage the stability of aircraft flight performance. Therefore, research on vibration suppression of SRM is fundamental [95]. The current vibration suppression technology is mainly achieved through algorithm optimization and external interference.

1) Algorithm Optimization: The traditional voltage single pulse drive method has been widely used in the SRM due to its simplicity and cost-effectiveness. However, a single pulse drive usually excites the natural frequency of the SRM, causing significant mechanical vibration.

The VC method achieves effective control and vibration reduction of SRM by designing a current controller that regulates the current [96]. The methods for reducing SRM vibration based on optimizing VC include designing a current controller with maximum torque current ratio [97], [98] and PWM technology [96], [99], [100]. The PWM method controls the waveform of the input voltage to include a unique frequency component higher than the driving frequency, thereby avoiding excitation of the natural resonance frequency when the voltage is turned OFF [53], [59].

The VC algorithm has been validated for its effective vibration reduction effect under high-speed performance. At a speed of 20 000 r/min and a torque of 16.2 N · m, the SRM using VC algorithm achieved vibration reduction compared to voltage single pulse drive [101].

In addition to improving the VC method, by adjusting the current distribution, the occurrence of resonance problems can be effectively reduced, and the stability and performance of the system can be improved [102], [103], [104]. In [105], a new current profile method was proposed. In [106], an optimization algorithm based on GA was introduced to achieve vibration attenuation and maintain reasonable copper loss. In [107] and [108], the MPT and FC method was proposed, which achieved the goal of minimizing torque and force ripple through online optimization of shared functions.

2) External Interference: When the radial vibration caused by electromagnetic fields can be accurately predicted, introducing new vibration signals for AVC can achieve lower net vibration, as shown in Fig. 23 [109]. The core idea of the AVC method is to adjust the reverse signal before vibration occurs to predict and suppress vibration. In [110], the complete peak acceleration characteristics were obtained through an improved least squares SVM and utilized AVC to suppress natural vibrations.

In addition to applying vibration, the vibration amplitude can also be controlled by controlling the rate of change of the applied

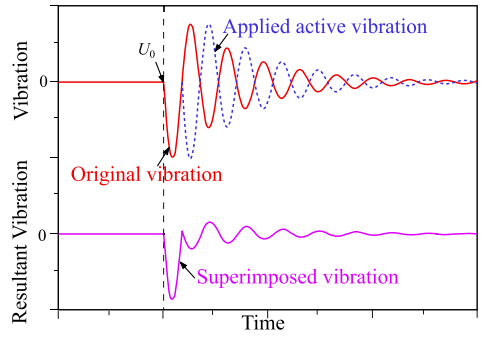

Fig. 23. AVC method [109].

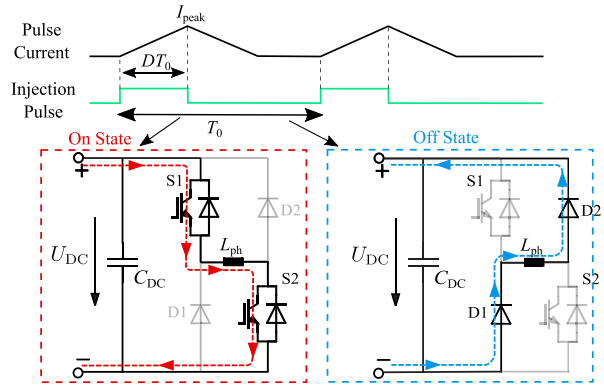

Fig. 24. Principle diagram of the pulse injection [119].

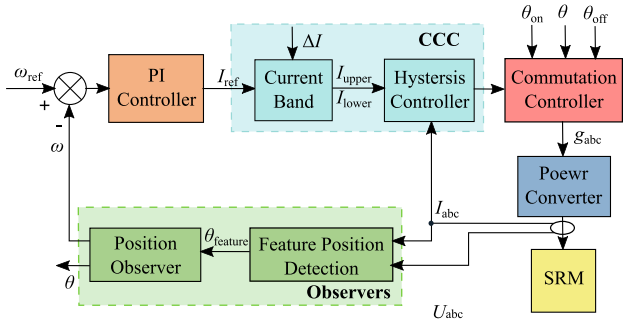

Fig. 25. Diagram of position sensorless control in [126].

phase voltage. At the beginning of demagnetization, applying negative voltage can shorten the demagnetization interval and suppress negative torque [111], [112].

In summary, most methods for reducing vibration come at the cost of sacrificing some efficiency. In order to achieve SRM research in the context of MEA, it is necessary to develop multi-objective optimization algorithms that balance performance and efficiency while optimizing vibration suppression. At the same time, a real-time monitoring and feedback system should be established to detect and adjust vibration conditions promptly to improve the stability and response speed of the system.

D. Position Sensorless Methods

The closed-loop position is an essential feature of the SRM speed control system. Traditionally, the rotor position is detected by mechanical position sensors. However, their presence undermines the advantages of SRM in terms of simple structure and adaptability to harsh environments. In addition, they reduce performance at high speeds and make the entire system susceptible to changes in temperature and operating conditions [113], [114]. Therefore, to achieve higher performance MEA machine control, sensorless control is a hot topic in SRM research. At present, research on sensorless methods is mainly divided into two categories based on the operating speed of machines, namely zero or low speed and medium to high speed.

1) Zero or Low-Speed Sensorless Method: Several methods exist for initial position detection of sensorless SRM, such as the phase current method, phase inductance method, and test coil method [115], [116]. In [117], the rotor position was estimated based on a convex function optimization algorithm. In [118], it was preferred to inject short-term high-frequency signals to capture the peak current of the phase and perform curve fitting to estimate the initial position.

The position sensorless control based on the pulse injection method has been widely studied in the low-speed operation of SRMs. The basic pulse injection principle diagram is shown in Fig. 24. The current methods include position estimation based on idle phase current injection [120], frequency conversion injection method [119], etc.

When the pulse frequency is low, the copper losses and maximum negative instantaneous torque in each pulse injection region will be higher. To solve this problem, pulse injection can be combined with SMC to keep the induced current at a minimum level throughout the entire idle phase [121]. Through the self-debugging process, the method in [122] has overcome the problem of offline measurement of magnetic parameters in traditional low-speed sensorless control methods.

2) Medium to High-Speed Sensorless Method: In the medium to high-speed stage, back EMF significantly affects the accuracy of the high-frequency pulse method. The medium to high-speed SRM with a sensorless control algorithm estimates the rotor position using reluctance and flux linkage information, along with current, etc. The position sensorless method based on signal processing has been tested on a starting/generator at 20 000 r/min and 150 kW, and its high accuracy has been demonstrated [123].

Sensorless position estimation methods based on virtual phase voltage and inductance have been proposed [124], [125]. However, these methods depend on the accuracy of flux linkage or phase inductance calculations and are limited when the flux linkage is saturated. At the same time, the flux linkage position relationship data table occupies a large amount of storage space.

Xiao et al. [126] designed a nonlinear state observer that avoids using 3-D magnetic properties, as shown in Fig. 25. In [127], the real-time rotor position was obtained by calculating the inductance value of the current overlapping phase and adjusting the phase inductance online. Ge et al. [128] have proposed a new continuous estimation method for SRM rotor position, which does not require any additional equipment or memory, and the maximum absolute estimation error was 1.67°.

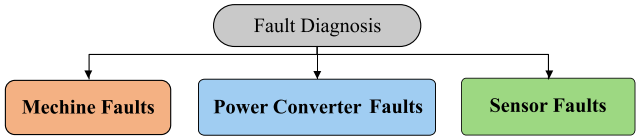

Fig. 26. Classifications of the fault diagnosis.

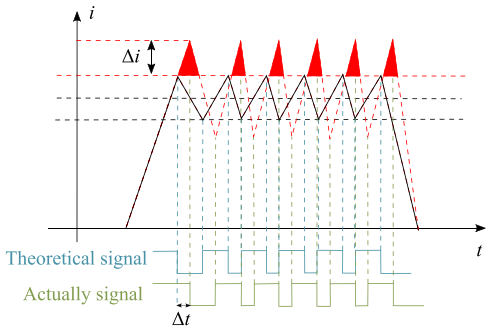

Fig. 27. Current overshoot caused by delay [134].

Currently, the sensorless control method for SRM is relatively mature and has been tested in large loads and wide speed ranges. However, due to the high demand for safety and reliability in MEA, further fault tolerance analysis and onboard experiments are necessary [79]. Looking ahead to the future, research on sensorless control of SRM positions can focus more on improving steady-state and dynamic performance and reducing machine parameter dependence to achieve more widespread applications.

V. Fault Diagnosis and Tolerant Control

A. Fault Diagnosis Method

The faults of the SRM system may lead to severe consequences, such as over voltage, over current, permanent insulation damage, cooling problems, decreased efficiency, control errors, and unstable machine operation [129]. Studying the fault diagnosis and tolerant control technology of SRM can reduce downtime caused by equipment failures, improve system reliability, extend equipment life, and provide essential guarantees for the stable and efficient operation of MEA.

The main sources of faults in the SRM system in MEA include machine faults, power converter faults, and sensor faults, as shown in Fig. 26. According to statistics, machine failures and power converter failures are the most common, accounting for about 40% and 35% [130].

1) Machine Faults: At present, the widely studied machine faults mainly focus on two types, namely, winding faults and mechanical faults.

1) Winding faults: Winding faults usually include open circuit and short circuit faults [131], which can be determined by current detection. As the ITSC inductance decreases, the decay time of the fault phase current after the circuit breaker also decreases. By monitoring the changes in all phase currents within the aligned rotor positions, ITSC can be diagnosed [132], [133]. Fig. 27 shows the actual current including overshoot caused by delay. When ITSC faults occur, these overshoots will significantly increase [134]. When a fault occurs, the symmetry of the phase current frequency characteristics will be disrupted, resulting in negative sequence and zero sequence components [135]. Therefore, the results of Fourier analysis can also be used for fault diagnosis [136], [137]. However, this method cannot respond quickly to faults online and has insufficient sensitivity in the initial stage of fault diagnosis. In addition, methods, such as the extended Kalman filter [138] and the current profile method [139] were proposed for diagnosing winding faults.
2) Mechanical faults: The mechanical faults of SRM usually refer to the problems related to the mechanical structure that occur during the operation of the machine, which may include bearing fault, insulation damage, rotor eccentricity, etc.

The diagnostic method for mechanical faults is usually based on the judgment of machine parameter values. Changes in current amplitude can identify eccentricity faults, while current trajectories can distinguish between static and dynamic eccentricity faults [140], [141]. Measured values of flux linkage connections in the coil can also provide information on the severity and direction of different eccentricity faults [142]. By integrating vibration and current signals, SRM bearing faults can also be effectively diagnosed [143].

In addition, the high-frequency pulse injection method can be used to detect insulation damage and poor coil contact [144]. By combining FEA and time-frequency analysis methods, more accurate fault localization and diagnosis can be provided [145].

2) Power Converter Faults: After a power device fault, the phase current of the faulty phase is severely distorted, and the torque ripple of the SRM increases. If the fault is not detected and diagnosed promptly, the performance and the service life of SRM will be seriously affected. From current researches, the main focus of power converter fault diagnosis is to study power switch faults and power diode faults.

According to the reliability study of SRM drivers, the open circuit and short circuit failure rates of power switches are 8.373×10^{-7}/h and 7.327×10^{-7}/h. The failure rates of freewheeling diodes in standard converters are 1.14×10^{-9}/h and 9.3312×10^{-10}/h [130].

By analyzing the abnormal changes in the current signal, it is possible to accurately detect faults in the internal components of the power converter. In [146], [147], and [148], the fault type and location are located by monitoring current errors.

The current spectrum analysis method can distinguish different fault characteristic frequencies by performing frequency domain analysis on the current signal. In [149] and [150], precise detection and localization of single-phase faults, multiphase faults, and midpoint open circuit faults were achieved based on current spectrum analysis.

In addition, the method based on high-frequency voltage signal injection can also achieve fast power transistor fault identification [151], [152]. This method has fast response speed and high detection accuracy and is suitable for real-time monitoring.

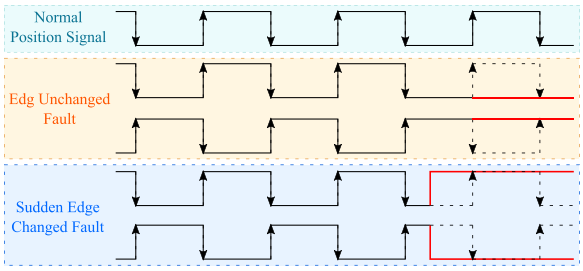

Fig. 28. Fault diagnosis for sensor pulse signals in [153].

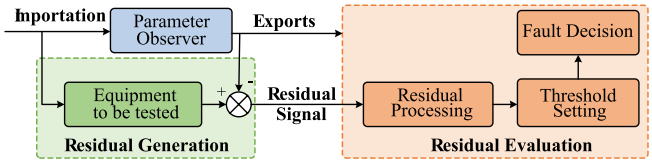

Fig. 29. Fault diagnosis based on mathematical models.

Although mature fault diagnosis techniques for power converters have been proposed, their practical application in MEA faces some limitations. For example, methods based on high-frequency signal injection may introduce additional interference in systems, requiring fine-tuning of the system to avoid misjudgment.

3) Sensor Faults: Sensors detect machine parameters and provide feedback to the controller for precise control. Faulty sensors can impair control performance and cause machine malfunction.

Sensor pulse signal analysis can diagnose fault moments through simple calculations and logical processing [154], [155]. In [153], a Grey prediction model was established to classify position signal faults into abrupt faults and edge invariant faults, as shown in Fig. 28. In [156], a phase inductance slope zero crossing detection scheme was established, which can capture at least one phase alignment position under regular operation and one phase fault-free operation.

4) Summary of Fault Diagnosis Methods: The existing SRM fault diagnosis methods can be roughly divided into mathematical model-based methods and signal processing-based methods.

The fault diagnosis method based on mathematical models usually establishes a complex mathematical model of the object to be tested, compares the theoretical values obtained by the parameter observer with the actual values obtained by the equipment to be tested under fault conditions, and calculates residuals. By comparing the residuals with the threshold, the fault is diagnosed, the specific principle is shown in Fig. 29. Common methods include parameter estimation [153], state estimation [154], [155], [157], etc.

The fault detection method based on signal processing is mainly based on the changes of characteristic signals in harmonic, amplitude, and other indicators, and processes the collected signals to extract and analyze fault features. The schematic diagram of this method is shown in Fig. 30. Among them, commonly used signal processing methods

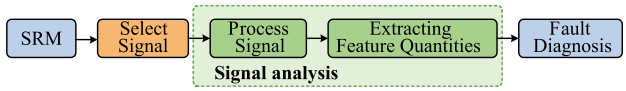

Fig. 30. Fault diagnosis based on signal processing.

include fast Fourier transform [132], [137], [155] and spectral analysis [134], [149].

The existing SRM fault diagnosis methods have good applicability in MEA and can effectively deal with machine faults, power converter faults, and sensor faults. However, these methods have certain limitations in terms of online response speed, anti-interference ability, and system complexity. Three main problems need to be solved in the current fault diagnosis methods for SRM as follows.

1) Low sensitivity: For short circuits with lower turns, the system may not be able to detect ITSC faults.
2) Interference from load changes: When facing load changes, the system may falsely report alarms without actual faults.
3) Dependence on control strategies: Existing diagnostic systems may overly rely on the control strategies used during machine operation.

By improving algorithms, adding sensitivity detection devices, and optimizing data processing methods, the fault diagnosis technology for SRM can be effectively improved, enhancing its accuracy and reliability.

B. Reliability Analysis and Fault Tolerant Control

The reliability analysis helps identify and correct potential weaknesses in machine design and production, thereby ensuring the stability and performance of the machine throughout its expected life cycle. When some components of the machine fail, fault tolerant control can help the machine avoid further damage and prevent potential safety accidents.

1) Reliability Analysis: The current reliability analysis of SRM systems mainly focuses on insulation reliability and power device reliability.

1) Insulation reliability: Insulation reliability issues are mainly caused by partial discharge resulting from stator terminal over-voltage or concentrated electric fields. The reliability analysis involves testing for PDIV according International Electrotechnical Commission (IEC 60034-18-41 and IEC 61934) [158], applying high-frequency pulse voltage, collecting partial discharge signals, and analyzing them with an oscilloscope after passing through a high-pass filter.
   Due to interference from phase to ground insulation, the phase to phase insulation test may fail prematurely [158], [159], as shown in the Fig. 31. Switching from a unipolar pulse to a bipolar pulse signal can effectively improve the reliability of testing [160].
   When conducting reliability analysis for SRMs used in MEA, it is essential to consider the impact of varying air

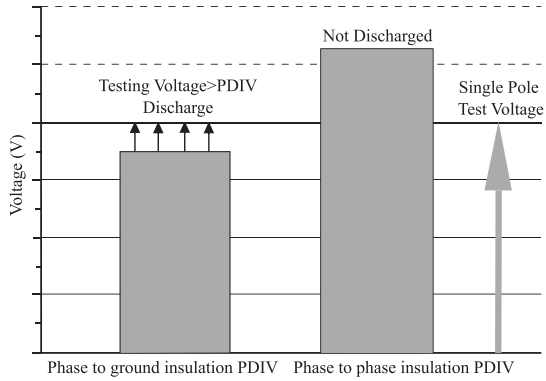

Fig. 31. Interference of phase to ground insulation discharge on testing [160].

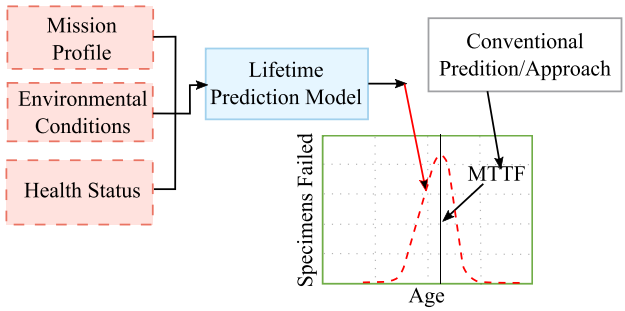

Fig. 32. Lifetime prediction model in [164].

pressures and humidity levels during different phases of flight.

Reliability analysis under different air pressures shows that as altitude increases and air pressure decreases, the insulation PDIV gradually decreases. From normal pressure to 50 kPa, the PDIV can decrease by up to 29.7% [160]. Similarly, reliability analysis under different humidity conditions indicates that as RH increases, insulation PDIV gradually decreases. When the RH increases from 40% to 95%, PDIV can be reduced by 15.9% [161].

2) Power device reliability: The reliability analysis of power converters focuses on prominent faulty power electronic components, such as semiconductor switches and capacitors [162], [163], whose main wear failure mechanism is thermal stress degradation [164]. By establishing corresponding failure criteria, current reliability analysis of power converters includes methods, such as combining Markov models [165], [166] or Bayesian networks [167].

In [164], a comprehensive physical failure model was established to focus on the reliability and lifespan factors, as shown in Fig. 32. The Weibull distribution provides a reliable framework for predicting insulation life, as follows:

$$F(\mathrm{t}) = 1 - \left(\exp\left(-\frac{\mathrm{t}}{\alpha} \right)^{\beta} \right) \tag{3}$$

where t is the fault time, β is the shape parameter, and α is the scale parameter.

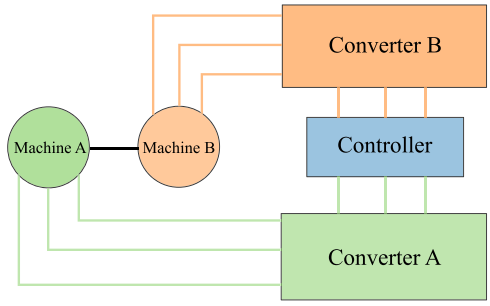

Fig. 33. Dual-redundancy drive with two machines [168].

By developing an advanced aging models, the lifespan of device could be accurately evaluated, which was different from traditional methods that only focused on average failure time without considering the variability of failure time.

Currently, most research on the reliability analysis of SRM for MEA applications relies on laboratory data, with inadequate feedback from practical applications. Future research should expand environmental adaptability analysis, improve reliability models, and strengthen practical application data collection to enhance SRM reliability in MEA.

2) Fault Tolerant Control: In order to ensure the normal operation of the system in the event of a failure, many advanced fault-tolerant design methods have been proposed and applied, mainly through the design of machine redundancy and power converter redundancy.

1) Machine redundancy: The machine redundancy method involves adding redundant components or systems to ensure the system can operate normally during a fault. By using SRM coaxial installation, machines of the same size and structure can be placed together, allowing for the continued operation of other machines in the event of a malfunction in one machine [168], [169], [170], as shown in Fig. 33. This method has been designed for the fuel pump driver of aircraft main engines with a 6/4 SRM [169]. In addition, in the machine design phase, two identical split winding can achieve fault tolerant operation for short or open circuit faults [171].

The machine redundancy method significantly improves system reliability, especially for critical areas requiring extremely high system fault tolerance. However, its high cost, increased complexity, weight, and space limitations are challenges that need to be carefully weighed and addressed.

2) Power converter redundancy: By introducing redundant components and structures in circuit design, power converter redundancy technology can effectively improve the fault tolerance of the system.

In traditional SRM drives, phase winding are typically connected in series. To enhance fault tolerance, faults in power switches, power diodes, and phase winding can be addressed by dividing the winding and creating nodes at different locations [172], [173]. In addition, by establishing different models for power switches, the system can switch to a

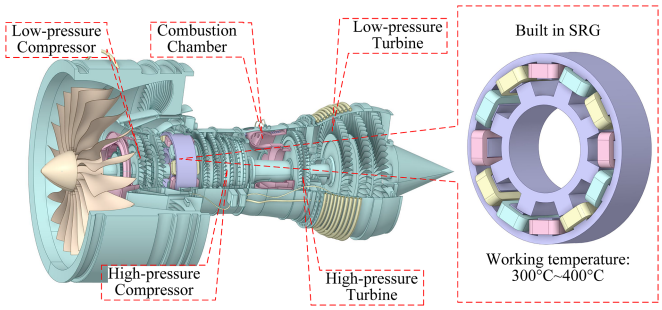

Fig. 34. Built-in SRG system.

backup switch module upon fault detection [174]. In the event of a power switch open circuit fault, the system can increase the current in the healthy channel, effectively managing the fault, as discussed in sources [175].

Compared to traditional power converters, multilevel converters have higher fault tolerance due to their ability to provide redundant operating modes with more semiconductor switches.

The fault tolerant control through multilevel power converters is mainly based on neutral point clamping level structures [176], [177], [178], [179]. The current path during faults can be reconfigured by using additional diodes and switches to avoid damaging other components [180]. However, as the number of switches increases, the probability of failure also increases, requiring more complex control and higher costs.

Machine redundancy offers robust fault tolerance but at the cost of increased complexity and weight, which may be restrictive in aerospace applications. In contrast, power converter redundancy, particularly with multilevel converters, provides scalable fault tolerance solutions, although with heightened complexity and cost considerations. Future research could optimize fault diagnosis algorithms, reduce system complexity, and integrate cost-effective redundancy solutions tailored to the unique demands of MEA propulsion systems.

VI. Applications and Challenges

Currently, SRM technology is not widely used in commercial aviation. However, its successful application in military aircraft has proven its viability in aerospace, specifically as a starting and power generation system. An aviation built-in SRG system includes high and low-pressure compressors, turbines, internal combustion chambers, and SRG, and it can withstand aviation high temperatures ranging from 300 °C to 400 °C, as shown in Fig. 34.

As technology advances, the design and implementation of SRMs continue to improve. For instance, the authors in [22] and [108] demonstrated the potential of SRMs through their high-speed 45 kW SRM, which utilized segmented pole rotor structures, unique materials, and iterative optimization programs based on FEA to achieve a wide range of constant power speeds and improve torque capability. Barzkar and Ghassemi [4] studied the use of SRM drivers in the MEA power system, while a four-phase 16/12 structure SRM, suitable for MEA systems, was introduced in [181]. This design aimed to achieve medium to high-speed power generation and low-speed high-torque starting, effectively mitigating torque ripple. The design has dual overload capabilities, providing 30 N· m of torque at 2200 r/min and 12 kW of power generation at 8000–12 000 r/min. Moreover, a 30 kW, 50 000 r/min SRM was designed for military aerospace applications in [14].

TABLE VI
Long Term Plan for MEA Machine Power Density Target [182]

Organization	Planned duration	Power density(kW/kg)
NASA	10 Years	>13
	15 Years	>16
Airbus	15 Years	10–15
U.S.Air Force	20 Years	>5

The current use of the SRM in the aviation industry presents a set of challenges that require consideration. These challenges include the following.

1) Efficiency and power density: The working principle of SRM results in significant losses under certain operating conditions, especially under partial load and low-speed operation. Based on the analysis of current research, the current SRM research can only achieve an efficiency level of 80%, and the development of power density is also limited.
   Currently, various organizations have set different power density targets for MEA machines in their long-term plans, as shown in Table VI [182]. The future goal is to improve materials and optimize structures, combined with new structures (such as DSSRM and PM-SRM) to increase the power density of SRM to a higher level and adopt advanced control algorithms to ensure low losses.
2) Noise and vibration: The noise and vibration generated by SRM during operation can affect passenger comfort and mechanical stability. The current measures include optimizing machine design (such as rotor and stator tooth profile design), researching higher performance vibration control strategies, and using vibration-absorbing materials to reduce noise and vibration.
3) Control accuracy: The nonlinear characteristics and torque ripple of SRM require precise control algorithms to ensure stable operation. For the current advanced algorithms of SRM, such as MPTC and intelligent algorithms, it is necessary to test them under higher load and speed conditions to verify their applicability to MEA. Meanwhile, developing high-performance digital signal processors is also crucial for implementing complex control strategies.
4) Thermal management: Although SRM can operate at higher temperatures, the compact space and limited heat dissipation capacity in aviation applications require efficient thermal management systems. The future thermal management system needs to be able to operate at high temperatures of 300 °C to 400 °C and maintain the machine temperature below 200 °C to ensure long-term stable operation of the equipment.

5) Reliability and safety requirements: The aircraft has extremely high requirements for the reliability and safety of machines, and any potential failure may lead to serious consequences. In the future, comprehensive testing and analysis are needed to reduce failure rates through redundant design and fault prediction techniques, ensuring the reliability and safety of critical applications.

VII. Conclusion

As the aviation industry moves towards higher energy efficiency, reliability, and safety, the concept of MEA has received widespread attention. As an emerging machine technology, the SRM has become a hot research topic in this field due to its unique advantages. In this article, we review the latest developments in the design, control, fault diagnosis, and tolerant control of SRM. By analyzing the research results of various indicators, such as power, torque, torque ripple, and efficiency, this article discusses the technical and experimental limitations of current research of SRM, evaluates the applicability and limitations of theoretical models in practical applications of MEA, and proposes future research directions that need to be focused on.

Although the application of SRM in the aviation industry is currently facing challenges, with the continuous progress of technology, it is expected to achieve a wider range of applications in the aviation industry in the future. Through research and optimization, SRM has the potential to become an efficient, reliable, and cost-effective machine solution in the aviation industry.

References

[1] G. Buticchi, P. Wheeler, and D. Boroyevich, "The more-electric aircraft and beyond," *Proc. IEEE*, vol. 111, no. 4, pp. 356–370, Apr. 2023.

[2] H. Ercan and M. Akin, "Performance analysis of electrical flight control actuation system in a commercial transport aircraft," *Aircr. Eng. Aerosp. Technol.*, vol. 94, no. 10, pp. 1671–1683, 2022.

[3] L. Ge, B. Burkhart, A. K. Hessling, H. Xu, and R. W. De Doncker, "Comprehensive performance comparison and optimization of single-pulse controlled SRGs for renewable electrical grids," in *2019 IEEE Appl. Power Electron. Conf. Expo.*, 2019, pp. 2632–2637.

[4] A. Barzkar and M. Ghassemi, "Components of electrical power systems in more and all-electric aircraft: A review," *IEEE Trans. Transport. Electrific.*, vol. 8, no. 4, pp. 4037–4053, Dec. 2022.

[5] P. Wheeler, "Technology for the more and all electric aircraft of the future," in *2016 IEEE Int. Conf. Automatica*, 2016, pp. 1–5.

[6] Y. Wang, S. Nuzzo, H. Zhang, W. Zhao, C. Gerada, and M. Galea, "Challenges and opportunities for wound field synchronous generators in future more electric aircraft," *IEEE Trans. Transport. Electrific.*, vol. 6, no. 4, pp. 1466–1477, Dec. 2020.

[7] E. B. Canfield and J. W. Summerford, "Variable speed constant frequency (VSCF) aircraft electrical power," Aerospace Meeting, SAE International, SAE Tech. Paper, 771002, Feb. 1977.

[8] C. Anghel, "Modeling and simulation of a power generation system with a high power generator," SAE AeroTech Congr. and Exhib., SAE Int., SAE Tech. Paper 2013-01-2126, Sep. 2013.

[9] A. C. Smith, M. F. Iacchetti, and P. M. Tuohy, "Feasibility study of an induction motor rim drive for an aircraft boundary-layer-ingestion fan," *J. Eng.*, vol. 2019, no. 17, pp. 4506–4510.

[10] P. Arumugam et al., "Permanent magnet starter-generator for aircraft application," in *Proc. SAE 2014 Aerosp. Syst. Technol. Conf.*, Sep. 2014, pp. 1–7.

[11] A. Yoon, F. Arastu, D. Lohan, J. Xiao, and K. Haran, "Direct-drive electric motor for STARC-ABL tail-cone propulsor," in *2019 AIAA/IEEE Electric Aircr. Technol. Symp.*, 2019, pp. 1–10.

[12] E. Richter and C. Ferreira, "Performance evaluation of a 250 kW switched reluctance starter generator," in *Proc. IAS'95 Conf. Rec. 1995 IEEE Ind. Appl. Conf. 30th IAS Annu. Meeting*, 1995, pp. 434–440.

[13] K. Kiyota and A. Chiba, "Design of switched reluctance motor competitive to 60-kW IPMSM in third-generation hybrid electric vehicle," *IEEE Trans. Ind. Appl.*, vol. 48, no. 6, pp. 2303–2309, Nov./Dec. 2012.

[14] S. MacMinn and W. Jones, "A very high speed switched-reluctance starter-generator for aircraft engine applications," in *Proc. IEEE Nat. Aerosp. Electron. Conf.*, 1989, vol. 4, pp. 1758–176.

[15] V. Madonna, P. Giangrande, and M. Galea, "Electrical power generation in aircraft: Review, challenges, and opportunities," *IEEE Trans. Transport. Electrific.*, vol. 4, no. 3, pp. 646–659, Sep. 2018.

[16] E. Sayed et al., "Review of electric machines in more-/hybrid-/turbo-electric aircraft," *IEEE Trans. Transport. Electrific.*, vol. 7, no. 4, pp. 2976–3005, Dec. 2021.

[17] L. Ge, B. Burkhart, and R. W. De Doncker, "Fast iron loss and thermal prediction method for power density and efficiency improvement in switched reluctance machines," *IEEE Trans. Ind. Electron.*, vol. 67, no. 6, pp. 4463–4473, Jun. 2020.

[18] N. Apostolidou and N. Papanikolaou, "Active power control of switched reluctance generator in more electric aircraft," *IEEE Trans. Veh. Technol.*, vol. 70, no. 12, pp. 12604–12616, Dec. 2021.

[19] J. K. Nøland, M. Leandro, J. A. Suul, M. Molinas, and R. Nilssen, "Electrical machines and power electronics for starter-generators in more electric aircrafts: A technology review," in *Proc. IECON 2019-45th Annu. Conf. IEEE Ind. Electron. Soc.*, 2019, pp. 6994–7001.

[20] R. Krishnan, D. Blanding, A. Bhanot, A. Staley, and N. Lobo, "High reliability SRM drive system for aerospace applications," in *Proc. IECON'03 29th Annu. Conf. IEEE Ind. Electron. Soc.*, 2003, pp. 1110–1115.

[21] C. Ferreira, S. Jones, W. Heglund, and W. Jones, "Detailed design of a 30-kW switched reluctance starter/generator system for a gas turbine engine application," *IEEE Trans. Ind. Appl.*, vol. 31, no. 3, pp. 553–561, May/Jun. 1995.

[22] J. B. Bartolo, M. Degano, J. Espina, and C. Gerada, "Design and initial testing of a high-speed 45-kW switched reluctance drive for aerospace application," *IEEE Trans. Ind. Electron.*, vol. 64, no. 2, pp. 988–997, Feb. 2017.

[23] J. B. Bartolo and C. Gerada, "The electromagnetic design of a high speed, 45 kW, switched reluctance machine having a novel rotor geometry for aerospace application," in *2014 Int. Conf. Elect. Mach.*, 2014, pp. 2513–2519.

[24] J. K. Nøland, M. Leandro, J. A. Suul, and M. Molinas, "High-power machines and starter-generator topologies for more electric aircraft: A technology outlook," *IEEE Access*, vol. 8, pp. 130104–130123, 2020.

[25] E. Sayed, M. H. Bakr, B. Bilgin, and A. Emadi, "Geometric optimization of switched reluctance motors using an invasive weed method," in *2018 IEEE Elect. Power Energy Conf.*, 2018, pp. 1–3.

[26] T. Burress and L. M. Tolbert, "A framework for multiple objective co-optimization of switched reluctance machine design and control," in *2021 IEEE Transp. Electrific. Conf. Expo*, 2021, pp. 1–6.

[27] J. Huang, J. Liu, L. Ge, Q. Zhao, X. Duan, and H. Meng, "Optimal design of double-stator switched reluctance machine with solution database method," in *2022 IEEE Transp. Electrific. Conf. Expo*, 2022, pp. 80–85.

[28] V. Wilson, P.G. Latha, and K. Vinida, "Improved two stage commutation for effective vibration reduction in switched reluctance motor using particle swarm optimization," in *2022 IEEE Int. Conf. Power Electron., Smart Grid, Renewable Energy*, 2022, pp. 1–6.

[29] H. Li, T. Liu, X. Wu, and Q. Chen, "A bearing fault diagnosis method based on enhanced singular value decomposition," *IEEE Trans. Ind. Informat.*, vol. 17, no. 5, pp. 3220–3230, May 2021.

[30] M. E. Abdollahi, N. Vaks, and B. Bilgin, "A multi-objective optimization framework for the design of a high power-density switched reluctance motor," in *2022 IEEE Transp. Electrific. Conf. Expo*, 2022, pp. 67–73.

[31] V. S. Nagarajan et al., "Design optimization of ferrite assisted synchronous reluctance motor using multi-objective differential evolution algorithm," *IEEE Trans. Ind. Electron.*, vol. 36, no. 1, pp. 219–239, Jan. 2017.

[32] Y. Hua, H. Zhu, M. Gao, and Z. Ji, "Multiobjective optimization design of permanent magnet assisted bearingless synchronous reluctance motor using NSGA-II," *IEEE Trans. Ind. Electron.*, vol. 68, no. 11, pp. 10477–10487, Nov. 2021.

[33] M. El-Nemr, M. Afifi, H. Rezk, and M. Ibrahim, "Finite element based overall optimization of switched reluctance motor using multi-objective genetic algorithm (NSGA-II)," *Mathematics*, vol. 9, no. 5, 2021, Art. no.576.

[34] E. C. Abunike, O. I. Okoro, and I. E. Davidson, "Finite element design and multi objective optimization of four pole reluctance motor based on NSGA-II intelligent algorithm," in *2021 IEEE AFRICON*, 2021, pp. 1–6.

[35] C. Huang, H. Yuan, and Y. Geng, "Multi-objective preference optimization method of permanent magnet assisted reluctance motor," in *2021 17th Int. Conf. Comput. Intell. Secur.*, 2021, pp. 413–419.

[36] G. Sun, S. Song, J. Jiang, L. Ge, and W. Liu, "Characteristics testing and torque control of switched reluctance machine in aero-engine shaft-line-embedded starter/generator," in *2022 IEEE Ind. Appl. Soc. Annu. Meeting*, 2022, pp. 1–6.

[37] W. Yan, H. Chen, S. Liao, Y. Liu, and H. Cheng, "Design of a low-ripple double-modular-stator switched reluctance machine for electric vehicle applications," *IEEE Trans. Transport. Electrific.*, vol. 7, no. 3, pp. 1349–1358, Sep. 2021.

[38] L. Maharjan et al., "Comprehensive report on design and development of a 100-kW DSSRM," *IEEE Trans. Transport. Electrific.*, vol. 4, no. 4, pp. 835–856, Dec. 2018.

[39] Y. Yang, N. Schofield, and A. Emadi, "Double-rotor switched reluctance machine (DRSRM)," *IEEE Trans. Energy Convers.*, vol. 30, no. 2, pp. 671–680, Jun. 2015.

[40] A. C. V. M. Norhisam, I. Aris, M. H. Marhaban, D. Ahmad, and M. Nirei, "Double-rotor switched reluctance machine (DRSRM): Fundamentals and magnetic circuit analysis," in *2011 IEEE Student Conf. Res. Develop.*, 2011, pp. 294–299.

[41] M. Vatani and M. Mirsalim, "The modular and crooked-tooth translator linear switched reluctance motor with a high-thrust per weight," *IEEE Trans. Transport. Electrific.*, vol. 7, no. 3, pp. 1359–1369, Sep. 2021.

[42] O. Gundogmus et al., "Acoustic noise mitigation in high pole count switched reluctance machines utilizing skewing method on stator and rotor poles," *IEEE Trans. Ind. Electron.*, vol. 69, no. 6, pp. 5581–5593, Jun. 2022.

[43] D. Marcsa and M. Kuczmann, "Design and control for torque ripple reduction of a 3-phase switched reluctance motor," *Comput. Math. Appl.*, vol. 74, no. 1, pp. 89–95, 2017.

[44] G. Guidkaya, E. D. K. Fankem, and J. Y. Effa, "A new rotor shape design of 6/2 switched reluctance motor: Comparative analysis of its chaotic behavior with other structures," *Elect. Eng. Technol*, vol. 16, no. 1, pp. 309–320, 2021.

[45] O. Gundogmus et al., "Acoustic noise mitigation of switched reluctance machines with windows on stator and rotor poles," *IEEE Trans. Ind. Appl.*, vol. 56, no. 4, pp. 3719–3730, Jul./Aug. 2020.

[46] G. J. Li, X. Y. Ma, G. W. Jewell, and Z. Q. Zhu, "Novel modular switched reluctance machines for performance improvement," *IEEE Trans. Energy Convers.*, vol. 33, no. 3, pp. 1255–1265, Sep. 2018.

[47] S. Mehta, M. A. Kabir, P. Pramod, and I. Husain, "Segmented rotor mutually coupled switched reluctance machine for low torque ripple applications," *IEEE Trans. Ind. Appl.*, vol. 57, no. 4, pp. 3582–3594, Jul./Aug. 2021.

[48] Z. Xu, J. Liu, M.-J. Kim, D.-H. Lee, and J.-W. Ahn, "Characteristics analysis and comparison of conventional and segmental rotor type 12/8 switched reluctance motors," *IEEE Trans. Ind. Appl.*, vol. 55, no. 3, pp. 3129–3137, May/Jun. 2019.

[49] E. F. Farahani, M. A. Jalali Kondelaji, and M. Mirsalim, "A new exterior-rotor multiple teeth switched reluctance motor with embedded permanent magnets for torque enhancement," *IEEE Trans. Magn.*, vol. 56, no. 2, Feb. 2020, Art. no.8100405.

[50] J. Ma et al., "Optimal design of an axial-flux switched reluctance motor with grain-oriented electrical steel," *IEEE Trans. Ind. Appl.*, vol. 53, no. 6, pp. 5327–5337, Nov./Dec. 2017.

[51] A. Ghaffarpour and M. Mirsalim, "Split-tooth double-rotor permanent magnet switched reluctance motor," *IEEE Trans. Transport. Electrific.*, vol. 8, no. 2, pp. 2400–2411, Jun. 2022.

[52] M. A. J. Kondelaji and M. Mirsalim, "Segmented-rotor modular switched reluctance motor with high torque and low torque ripple," *IEEE Trans. Transport. Electrific.*, vol. 6, no. 1, pp. 62–72, Mar. 2020.

[53] W. Ding, H. Fu, and Y. Hu, "Characteristics assessment and comparative study of a segmented-stator permanent-magnet hybrid-excitation SRM drive with high-torque capability," *IEEE Trans. Power Electron.*, vol. 33, no. 1, pp. 482–500, Jan. 2018.

[54] F. Yu et al., "Design and multiobjective optimization of a double-stator axial flux SRM with full-pitch winding configuration," *IEEE Trans. Transport. Electrific.*, vol. 8, no. 4, pp. 4348–4364, Dec. 2022.

[55] S. Ullah, S. P. McDonald, R. Martin, M. Benarous, and G. J. Atkinson, "A permanent magnet assist, segmented rotor, switched reluctance drive for fault tolerant aerospace applications," *IEEE Trans. Ind. Appl.*, vol. 55, no. 1, pp. 298–305, Jan./Feb. 2019.

[56] M. A. J. Kondelaji, E. F. Farahani, and M. Mirsalim, "Performance analysis of a new switched reluctance motor with two sets of embedded permanent magnets," *IEEE Trans. Energy Convers.*, vol. 35, no. 2, pp. 818–827, Jun. 2020.

[57] E. F. Farahani, M. A. J. Kondelaji, and M. Mirsalim, "An innovative hybrid-excited multi-tooth switched reluctance motor for torque enhancement," *IEEE Trans. Ind. Electron.*, vol. 68, no. 2, pp. 982–992, Feb. 2021.

[58] W. Ding, H. Bian, K. Song, Y. Li, and K. Li, "Enhancement of a 12/4 hybrid-excitation switched reluctance machine with both segmented-stator and rotor," *IEEE Trans. Ind. Electron.*, vol. 68, no. 10, pp. 9229–9241, Oct. 2021.

[59] M. A. J. Kondelaji and M. Mirsalim, "A novel hybrid-excited modular variable reluctance motor for electric vehicle applications: Analysis, comparison, and implementation," *AUT J. Elect. Eng.*, vol. 54, no. 1, pp. 45–54, 2019.

[60] Q. Li, W. Sun, L. Sun, and L. Li, "Rotor segment split and its optimization of axial-field dual-rotor segmented switched reluctance machine," in *Energy Rep.*, vol. 6, pp. 1144–1150, 2020. Proc. 7th Int. Conf. Power Energy Syst. Eng..

[61] L. Ge, I. Ralev, A. K. Hessling, S. Song, and R. W. De Doncker, "A simple reluctance calibration strategy to obtain the flux-linkage characteristics of switched reluctance machines," *IEEE Trans. Power Electron.*, vol. 35, no. 3, pp. 2787–2798, Mar. 2020.

[62] S. Song, M. Zhang, and L. Ge, "A new decoupled analytical modeling method for switched reluctance machine," *IEEE Trans. Magn.*, vol. 51, no. 3, Mar. 2015, Art. no. 8100504.

[63] A. Asok and N. P. Kumar, "Finite element-based dynamic eccentricity fault analysis in switched reluctance motor using machine learning approach," in *2023 7th Int. Conf. Comput. Appl. Elect. Eng.-Recent Adv.*, 2023, pp. 1–6.

[64] Y. Wu, Z. Li, S. Wang, L. Li, C. Gan, and J. Sun, "Angle position compensation control strategy for high-speed power generation of aerospace integrated switched reluctance starting/generating system," *IEEE Trans. Emerg. Sel. Topics Power Electron.*, vol. 11, no. 6, pp. 5690–5700, Dec. 2023.

[65] A. K. Sahu, A. Emadi, and B. Bilgin, "Noise and vibration in switched reluctance motors: A review on structural materials, vibration dampers, acoustic impedance, and noise masking methods," *IEEE Access*, vol. 11, pp. 27702–27718, 2023.

[66] S. S. Ahmad and G. Narayanan, "Predictive control based constant current injection scheme for characterization of switched reluctance machine," *IEEE Trans. Ind. Appl.*, vol. 54, no. 4, pp. 3383–3392, Jul./Aug. 2018.

[67] S. S. Ahmad, M. Thirumalasetty, and G. Narayanan, "Predictive current control of switched reluctance machine for accurate current tracking to enhance torque performance," *IEEE Trans. Ind. Appl.*, vol. 60, no. 1, pp. 1837–1848, Jan./Feb. 2024.

[68] M. Pereira and R. E. Araújo, "Model-free finite-set predictive current control with optimal cycle time for a switched reluctance motor," *IEEE Trans. Ind. Electron.*, vol. 70, no. 8, pp. 8355–8364, Aug. 2023.

[69] R. Abdel-Fadil and L. Számel, "Enhancement of the switched reluctance motor performance for electric vehicles applications using predictive current control," in *2018 Int. IEEE Conf. Workshop Óbuda Elect. Power Eng.*, 2018, pp. 000195–000200.

[70] M. Deepak, G. Janaki, and C. Bharatiraja, "Model predictive current control improved performance on SRM drive for electric vehicles," in *2023 IEEE Int. Transp. Electrific. Conf.*, 2023, pp. 1–6.

[71] G. Jie and G. Bing, "Axial switched reluctance wheel motor control system with the direct torque based on fractional order sliding mode," in *2019 Chin. Control Decis. Conf.*, 2019, pp. 2195–2200.

[72] S. B. Dhale, B.-N. Mobarakeh, S. Nalakath, and A. Emadi, "Digital sliding mode based model-free PWM current control of switched reluctance machines," *IEEE Trans. Ind. Electron.*, vol. 69, no. 9, pp. 8760–8769, Sep. 2022.

[73] H. M. Ben Salem, I. Bahri, H. Maamri, and N. Derbel, "A second-order sliding mode control of switched reluctance motor," *Electric Power Compon. Syst.*, vol. 48, no. 6/7, pp. 640–651, 2020.

[74] G. Fang et al., "An intersection-method-based current controller for switched reluctance machines with robust tracking performance," *IEEE Trans. Transport. Electrific.*, vol. 7, no. 4, pp. 2822–2834, Dec. 2021.
[75] J. Liu, G. Wang, D. Liu, and Y. Fan, "An improved deadbeat control scheme for unipolar sinusoidal current excited switched reluctance motor drives," *IEEE Trans. Emerg. Sel. Topics Power Electron.*, vol. 11, no. 2, pp. 1589–1603, Apr. 2023.
[76] R. R. C. Reis, M. L. M. Kimpara, L. Galotto, and J. O. P. Pinto, "Genetic algorithm-based commutation angle control for torque ripple mitigation in switched reluctance motor drives," *IEEE Access*, vol. 11, pp. 97331–97339, 2023.
[77] Y. Cai, Y. Wang, H. Xu, S. Sun, C. Wang, and L. Sun, "Research on rotor position model for switched reluctance motor using neural network," *IEEE/ASME Trans. Mechatron.*, vol. 23, no. 6, pp. 2762–2773, Dec. 2018.
[78] H. Alharkan, S. Saadatmand, M. Ferdowsi, and P. Shamsi, "Optimal tracking current control of switched reluctance motor drives using reinforcement q-learning scheduling," *IEEE Access*, vol. 9, pp. 9926–9936, 2021.
[79] D. Mohanraj, J. Gopalakrishnan, B. Chokkalingam, and J. O. Ojo, "An enhanced model predictive direct torque control of SRM drive based on a novel modified switching strategy for low torque ripple," *IEEE Trans. Emerg. Sel. Topics Power Electron.*, vol. 12, no. 2, pp. 2203–2213, Apr. 2024.
[80] N. Yan, X. Cao, and Z. Deng, "Direct torque control for switched reluctance motor to obtain high torque ampere ratio," *IEEE Trans. Ind. Electron.*, vol. 66, no. 7, pp. 5144–5152, Jul. 2019.
[81] S. Song, G. Fang, R. Hei, J. Jiang, R. Ma, and W. Liu, "Torque ripple and efficiency online optimization of switched reluctance machine based on torque per ampere characteristics," *IEEE Trans. Power Electron.*, vol. 35, no. 9, pp. 9608–9616, Sep. 2020.
[82] Q. Sun, J. Wu, and C. Gan, "Optimized direct instantaneous torque control for SRMs with efficiency improvement," *IEEE Trans. Ind. Electron.*, vol. 68, no. 3, pp. 2072–2082, Mar. 2021.
[83] L. Ge, J. Zhong, Q. Cheng, Z. Fan, S. Song, and R. W. De Doncker, "Model predictive control of switched reluctance machines for suppressing torque and source current ripples under bus voltage fluctuation," *IEEE Trans. Ind. Electron.*, vol. 70, no. 11, pp. 11013–11021, Nov. 2023.
[84] L. Ge, J. Zhong, J. Huang, and S. Song, "Model predictive torque control of switched reluctance machine based on torque-balanced measurement and flux-based torque estimation," in *2021 24th Int. Conf. Elect. Mach. Syst.*, 2021, pp. 867–872.
[85] L. Ge et al., "A composite model predictive control method of SRMs with PWM-based signal for torque ripple suppression," *IEEE Trans. Transp. Electrific.*, vol. 10, no. 2, pp. 2469–2478, Jun. 2024.
[86] L. Ge et al., "Model predictive control of SRMs based on modified multilevel power converter," *IEEE Trans. Transport. Electrific.*, 2023, to be published, doi: 10.1109/TTE.2023.3343431.
[87] L. Ge, J. Zhong, J. Huang, N. Jiao, S. Song, and R. W. De Doncker, "A novel model predictive torque control of SRMs with low measurement effort," *IEEE Trans. Ind. Electron.*, vol. 70, no. 4, pp. 3561–3570, Apr. 2023.
[88] H. Li, B. Bilgin, and A. Emadi, "An improved torque sharing function for torque ripple reduction in switched reluctance machines," *IEEE Trans. Power Electron.*, vol. 34, no. 2, pp. 1635–1644, Feb. 2019.
[89] Z. Xia, B. Bilgin, S. Nalakath, and A. Emadi, "A new torque sharing function method for switched reluctance machines with lower current tracking error," *IEEE Trans. Ind. Electron.*, vol. 68, no. 11, pp. 10612–10622, Nov. 2021.
[90] L. Ge et al., "Model predictive control of switched reluctance machines with online torque sharing function based on optimal flux-linkage curve," *IEEE Trans. Transport. Electrific.*, early access, 2023Oct. 16, doi: 10.1109/TTE.2023.3324707.
[91] F. Qi, A. Stippich, I. Ralev, A. Klein-Hessling, and R. W. De Doncker, "Model predictive control of a switched reluctance machine for guaranteed overload torque," *IEEE Trans. Ind. Appl.*, vol. 55, no. 2, pp. 1321–1331, Mar./Apr. 2019.
[92] Z. Xia, G. Fang, D. Xiao, A. Emadi, and B. Bilgin, "An online torque sharing function method involving current dynamics for switched reluctance motor drives," *IEEE Trans. Transp. Electrific.*, vol. 9, no. 1, pp. 534–548, Mar. 2023.
[93] S. Song, R. Hei, R. Ma, and W. Liu, "Model predictive control of switched reluctance starter/generator with torque sharing and compensation," *IEEE Trans. Transp. Electrific.*, vol. 6, no. 4, pp. 1519–1527, Dec. 2020.
[94] L. Ge, J. Guo, C. Gong, G. Zhang, X. Ding, and S. Song, "Model predictive torque control of switched reluctance machines with torque sharing function and PWM control signals based on linear polynomial fitting," *IEEE Trans. Power Electron.*, Aug. 16, 2024, doi: 10.1109/TPEL.2024.3444891.
[95] B. Bilgin et al., "Making the case for switched reluctance motors for propulsion applications," *IEEE Trans. Veh. Technol.*, vol. 69, no. 7, pp. 7172–7186, Jul. 2020.
[96] K. Aiso and K. Akatsu, "High speed SRM using vector control for electric vehicle," *CES Trans. Elect. Machines Syst.*, vol. 4, no. 1, pp. 61–68, 2020.
[97] N. Nakao and K. Akatsu, "Vector control for switched reluctance motor drives using an improved current controller," in *2014 IEEE Energy Convers. Congr. Expo.*, 2014, pp. 1379–1386.
[98] N. Nakao and K. Akatsu, "Vector control specialized for switched reluctance motor drives," in *2014 Int. Conf. Elect. Mach.*, 2014, pp. 943–949.
[99] A. Tanabe and K. Akatsu, "Vibration reduction method in SRM with a smoothing voltage commutation by PWM," in *2015 9th Int. Conf. Power Electron. ECCE Asia*, 2015, pp. 600–604.
[100] A. Zhu, P. Liu, J. Yu, C. Liu, and K. Wang, "Research on the effect of pulse width modulation frequency on radial force and vibration of switched reluctance motor," in *2019 22nd Int. Conf. Elect. Mach. Syst.*, 2019, pp. 1–6.
[101] K. Aiso, M. Takahashi, and K. Akatsu, "Study of high speed SRM using vector control for electric vehicle," in *2019 10th Int. Conf. Power Electron. ECCE Asia*, 2019, pp. 1–7.
[102] M. L. M. Kimpara, R. R. C. Reis, L. E. B. Da Silva, J. O. P. Pinto, and B. Fahimi, "A two-step control approach for torque ripple and vibration reduction in switched reluctance motor drives," *IEEE Access*, vol. 10, pp. 82106–82118, 2022.
[103] X. Guo, R. Zhong, M. Zhang, D. Ding, and W. Sun, "Resonance reduction by optimal switch angle selection in switched reluctance motor," *IEEE Trans. Ind. Electron.*, vol. 67, no. 3, pp. 1867–1877, Mar. 2020.
[104] M. Divandari and A. Dadpour, "Radial force and torque ripple optimization for acoustic noise reduction of SRM drives via fuzzy logic control," in *2010 9th IEEE/IAS Int. Conf. Ind. Appl.*, 2010, pp. 1–6.
[105] M. Kawa, K. Kiyota, J. Furqani, and A. Chiba, "Acoustic noise reduction of a high-efficiency switched reluctance motor for hybrid electric vehicles with novel current waveform," *IEEE Trans. Ind. Appl.*, vol. 55, no. 3, pp. 2519–2528, May/Jun. 2019.
[106] S. Shin, N. Kawagoe, T. Kosaka, and N. Matsui, "Study on commutation control method for reducing noise and vibration in SRM," in *2017 20th Int. Conf. Elect. Mach. Syst.*, 2017, pp. 1–6.
[107] L. Ge, Z. Fan, N. Du, J. Huang, D. Xiao, and S. Song, "Model predictive torque and force control for switched reluctance machines based on online optimal sharing function," *IEEE Trans. Power Electron.*, vol. 38, no. 10, pp. 12359–12364, Oct. 2023.
[108] L. Ge, R. Yuan, Q. Cheng, J. Zhong, C. Bao, and S. Song, "Model predictive torque and force control of an switched reluctance machine," in *2021 IEEE Int. Conf. Predictive Control Elect. Drives Power Electron.*, 2021, pp. 280–284.
[109] M. L. M. Kimpara et al., "Active cancellation of vibration in switched reluctance motor using mechanical impulse response method," *IEEE Trans. Energy Convers.*, vol. 34, no. 3, pp. 1358–1368, Sep. 2019.
[110] X. Guo, R. Zhong, M. Zhang, D. Ding, and W. Sun, "Improved model of radial vibration in switched reluctance motor including magnetic saturation," *CES Trans. Elect. Mach. Syst.*, vol. 2, no. 4, pp. 363–370, 2018.
[111] A. Malekipour, S. M. S. Nejad, and A. Rashidi, "Vibration reduction of SRM through controlling the average of applied demagnetization voltage," *IEEE Trans. Energy Convers.*, vol. 36, no. 3, pp. 1756–1765, Sep. 2021.
[112] Z. Sadeghi, S. M. S. Nejad, A. Rashidi, and M. Shahparasti, "Fast demagnetization and vibration reduction in switched reluctance motor drive system," *IEEE Access*, vol. 9, pp. 110904–110915, 2021.
[113] L. Yu, Z. Zhang, D. Gerada, and C. Gerada, "Performance comparison of doubly salient reluctance generators for high-voltage DC power system of more electric aircraft," in *2018 IEEE Int. Conf. Elect. Syst. Aircr., Railway, Ship Propulsion Road Veh. Int. Transp. Electrific. Conf.*, 2018, pp. 1–6.
[114] L. Ge, J. Guo, J. Huang, and S. Song, "Research on the smooth switching strategy of switched reluctance starter/ generator for more electric aircraft," in *2022 25th Int. Conf. Elect. Mach. Syst.*, 2022, pp. 1–6, doi: 10.1109/ICEMS56177.2022.9983147.

[115] L. He, H. Sun, J. Gao, and J. Bai, "A new method to detect the initial position for sensorless SRM," in *2011 Int. Conf. Electron., Commun. Control*, 2011, pp. 2450–2453.

[116] L. Ge et al., "A sensorless heavy load starting control method for srms with residual inductance calculation and polynomial fitting," *IEEE Trans. Ind. Electron.*, early access, Jul. 15, 2024, doi: 10.1109/TIE.2024.3413819.

[117] L. Ge, H. Xu, Z. Guo, S. Song, and R. W. De Doncker, "An optimization-based initial position estimation method for switched reluctance machines," *IEEE Trans. Power Electron.*, vol. 36, no. 11, pp. 13285–13292, Nov. 2021.

[118] S. K. Singh, A. K. Rana, and A. V. R. Teja, "High resolution initial rotor position estimation of SRM using peak current detection," in *Proc. IECON 2021, 47th Annu. Conf. IEEE Ind. Electron. Soc.*, 2021, pp. 1–6.

[119] J. Cai, Y. Yan, W. Zhang, and X. Zhao, "A reliable sensorless starting scheme for SRM with lowered pulse injection current influences," *IEEE Trans. Instrum. Meas.*, vol. 70, Nov. 2020, Art. no. 1003209, doi: 10.1109/TIM.2020.3040990.

[120] H. Chen, R. Nie, J. Gu, S. Yan, and R. Zhao, "Efficiency optimization strategy for switched reluctance generator system with position sensorless control," *IEEE/ASME Trans. Mechatron.*, vol. 26, no. 1, pp. 469–479, Feb. 2021.

[121] D. Xiao et al., "Induced current reduction in position-sensorless SRM drives using pulse injection," *IEEE Trans. Ind. Electron.*, vol. 70, no. 5, pp. 4620–4630, May 2023.

[122] D. Xiao, J. Ye, G. Fang, Z. Xia, X. Wang, and A. Emadi, "A regional phase-locked loop-based low-speed position-sensorless control scheme for general-purpose switched reluctance motor drives," *IEEE Trans. Power Electron.*, vol. 37, no. 5, pp. 5859–5873, May 2022.

[123] S. Wang, Z. Hu, and X. Cui, "High-precision sensorless control based on magnetic flux/current method for SRM starting/generating system," in *Proc. IECON 2020 46th Annu. Conf. IEEE Ind. Electron. Soc.*, 2020, pp. 251–258.

[124] W. Ding and K. Song, "Position sensorless control of switched reluctance motors using reference and virtual flux linkage with one-phase current sensor in medium and high speed," *IEEE Trans. Ind. Electron.*, vol. 67, no. 4, pp. 2595–2606, Apr. 2020.

[125] Q. Sun, T. Lan, X. Liu, S. Li, F. Niu, and C. Gan, "Linear inductance model reshaping-based sensorless position estimation method for SRM with antimagnetic saturation capability," *IEEE Trans. Emerg. Sel. Topics Power Electron.*, vol. 11, no. 5, pp. 4799–4807, Oct. 2023.

[126] D. Xiao, J. Ye, G. Fang, Z. Xia, X. Wang, and A. Emadi, "Improved feature-position-based sensorless control scheme for SRM drives based on nonlinear state observer at medium and high speeds," *IEEE Trans. Power Electron.*, vol. 36, no. 5, pp. 5711–5723, May 2021.

[127] C. Gan, F. Meng, Z. Yu, R. Qu, Z. Liu, and J. Si, "Online calibration of sensorless position estimation for switched reluctance motors with parametric uncertainties," *IEEE Trans. Power Electron.*, vol. 35, no. 11, pp. 12307–12320, Nov. 2020.

[128] L. Ge, J. Zhong, C. Bao, S. Song, and R. W. De Doncker, "Continuous rotor position estimation for SRM based on transformed unsaturated inductance characteristic," *IEEE Trans. Power Electron.*, vol. 37, no. 1, pp. 37–41, Jan. 2022.

[129] C. Gan, Y. Chen, R. Qu, Z. Yu, W. Kong, and Y. Hu, "An overview of fault-diagnosis and fault-tolerance techniques for switched reluctance machine systems," *IEEE Access*, vol. 7, pp. 174822–174838, 2019.

[130] N. Ali and M. Narimani, "Fault-tolerant SRM drives–A review," *IEEE Trans. Power Electron.*, vol. 39, no. 8, pp. 10261–10275, Aug. 2024.

[131] N. Ali, Q. Gao, and K. Ma, "Diagnosis of power transistors open-and short-circuit faults in SRM drives through current error analysis," in Proc. *2021 IEEE 13th Int. Symp. Diagnostics Elect. Mach., Power Electron. Drives*, 2021, pp. 221–226.

[132] M. Alam, N. Gugulothu, and S. Payami, "A novel diagnosis method for interturn short-circuits in SRMs by tracking post turn-off phase currents under current chopping control," *IEEE Trans. Ind. Electron.*, vol. 71, no. 1, pp. 49–58, Jan. 2024.

[133] G. Han, H. Chen, and X. Shi, "Modelling, diagnosis, and tolerant control of phase-to-phase fault in switched reluctance machine," *IET Electric Power Appl.*, vol. 11, no. 9, pp. 1527–1537, 2017.

[134] P. Zhang, K. Li, S. Yu, and D. Yu, "A novel fault diagnosis technique of interturn short-circuit fault for SRM in current chopper mode," *IEEE Trans. Ind. Electron.*, vol. 69, no. 3, pp. 3037–3046, Mar. 2022.

[135] M. Alam and S. Payami, "A novel control-independent online fault diagnosis of interturn short circuits in SRMs using signal injection technique," *IEEE Trans. Ind. Electron.*, vol. 70, no. 3, pp. 2157–2167, Mar. 2023.

[136] H. Chen et al., "Diagnosis of interturn short-circuit of SRM based on ratio of current components," *IEEE Trans. Transp. Electrific.*, vol. 9, no. 2, pp. 3319–3327, Jun. 2023.

[137] L. Xiao, H. Sun, F. Gao, S. Hou, and L. Li, "A new diagnostic method for winding short-circuit fault for SRM based on symmetrical component analysis," *Chin. J. Elect. Eng.*, vol. 4, no. 1, pp. 74–82, 2018.

[138] S. R. Khayam Hoseini, E. Farjah, T. Ghanbari, and H. Givi, "Extended Kalman filter-based method for inter-turn fault detection of the switched reluctance motors," *IET Electric Power Appl.*, vol. 10, no. 8, pp. 714–722, 2016.

[139] P. Dubravka, P. Rafajdus, P. Makys, and L. Szabo, "Control of switched reluctance motor by current profiling under normal and open phase operating condition," *IET Electric Power Appl.*, vol. 11, no. 4, pp. 548–556, 2017.

[140] A. V. Reddy and B. M. Kumar, "Analysis of various levels of air gap eccentricity faults in switched reluctance motor," in *2018 2nd Int. Conf. Electron., Commun. Aerosp. Technol.*, 2018, pp. 516–521.

[141] M. Alam, V. Shah, and S. Payami, "Online fault diagnosis of static and dynamic eccentricity in switched reluctance motors using parks vector algorithm," in *Proc. 10th Int. Conf. Power Electron., Mach. Drives*, 2020, vol. 2020, pp. 885–889.

[142] R. Moradi and A. Hajihosseinlu, "A novel method for diagnosis and analysis of rotor faults in switched reluctance motor," in *Proc. 5th Annu. Int. Power Electron., Drive Syst. Technol. Conf.*, 2014, pp. 329–333.

[143] X. Wang, S. Lu, K. Chen, Q. Wang, and S. Zhang, "Bearing fault diagnosis of switched reluctance motor in electric vehicle powertrain via multisensor data fusion," *IEEE Trans. Ind. Informat.*, vol. 18, no. 4, pp. 2452–2464, Apr. 2022.

[144] H. Torkaman and E. Afjei, "Comprehensive detection of eccentricity fault in switched reluctance machines using high-frequency pulse injection," *IEEE Trans. Power Electron.*, vol. 28, no. 3, pp. 1382–1390, Mar. 2013.

[145] I. Bouchareb, A. Bentounsi, A. Lebaroud, and B. Batoun, "Three dimension time-frequency approach for diagnosing eccentricity faults in switched reluctance motor," in *2012 6th Int. Conf. Sci. Electron., Technol. Inf. Telecommun.*, 2012, pp. 740–747.

[146] G. Han, H. Chen, and G. Guan, "Generalised fault diagnostic method for power transistors in asymmetric half-bridge power converter of SRM drive," *IET Electric Power Appl.*, vol. 13, no. 2, pp. 168–180, 2019.

[147] D. Sun, Y. Hu, and Z. Kang, "Modified fault diagnosis method of power converter in SRM based on bridge current reconstruction scheme," in *2021 IEEE 4th Student Conf. Electric Mach. Syst.*, 2021, pp. 1–6.

[148] H. Chen, C. Fang, G. Guan, and N. Parspour, "Fault diagnosis for power converter in SRM drives based on current prediction," *IEEE Trans. Ind. Electron.*, vol. 69, no. 12, pp. 13576–13585, Dec. 2022.

[149] M. Guan, C. Liu, P. Liu, and X. Sun, "Fault diagnosis scheme for open-circuit fault in n 2 converter of six-phase SRM using midpoint current spectrum analysis," *IEEE Access*, vol. 10, pp. 105983–105992, 2022.

[150] C. Gan, J. Wu, S. Yang, Y. Hu, W. Cao, and J. Si, "Fault diagnosis scheme for open-circuit faults in switched reluctance motor drives using fast fourier transform algorithm with bus current detection," *IET Power Electron.*, vol. 9, no. 1, pp. 20–30, 2016.

[151] N. Ali, Q. Gao, P. Sovicka, P. Makys, M. Stulrajter, and K. Ma, "Power converter fault detection and isolation using high-frequency voltage injection in switched reluctance motor drives for automotive applications," *IEEE Trans. Emerg. Sel. Topics Power Electron.*, vol. 10, no. 3, pp. 3395–3408, Jun. 2022.

[152] N. Ali, Q. Wang, Q. Gao, and K. Ma, "Fast detection of power transistor faults in SRM drives based on transient pulse injection," *IEEE Trans. Emerg. Sel. Topics Power Electron.*, vol. 11, no. 5, pp. 5256–5267, Oct. 2023.

[153] X. Sun, Y. Xiong, M. Yao, and J. Wu, "High fault-tolerance evaluation on position signal for switched reluctance motor drives," *IEEE Trans. Energy Convers.*, vol. 37, no. 3, pp. 1844–1853, Sep. 2022.

[154] H. Chen, G. Guan, G. Han, and H. Chen, "Fault diagnosis and tolerant control strategy for position sensors of switched reluctance starter/generator systems," *IEEE Trans. Transp. Electrific.*, vol. 6, no. 4, pp. 1508–1518, Dec. 2020.

[155] J. Cai and X. Zhao, "Synthetic hybrid-integral-threshold logic-based position fault diagnosis scheme for SRM drives," *IEEE Trans. Instrum. Meas.*, vol. 70, Oct. 2020, Art. no. 1500608, doi: 10.1109/TIM.2020.3031357.
[156] J. Cai, Z. Liu, and Y. Zeng, "Aligned position estimation based fault-tolerant sensorless control strategy for SRM drives," *IEEE Trans. Power Electron.*, vol. 34, no. 8, pp. 7754–7762, Aug. 2019.
[157] M. Tursini, M. Villani, G. Fabri, and L. Di Leonardo, "A switched-reluctance motor for aerospace application: Design, analysis and results," *Electric Power Syst. Res.*, vol. 142, pp. 74–83, 2017.
[158] M. Tozzi, A. Cavallini, and G. C. Montanari, "Monitoring off-line and on-line PD under impulsive voltage on induction motors — Part 1: Standard procedure," *IEEE Elect. Insul. Mag.*, vol. 26, no. 4, pp. 16–26, Jul./Aug. 2010.
[159] A. Cavallini, E. Lindell, G. C. Montanari, and M. Tozzi, "Off-line PD testing of converter-fed wire-wound motors: When IEC TS 60034-18-41 may fail?," *IEEE Trans. Dielectr. Elect. Insul.*, vol. 17, no. 5, pp. 1385–1395, Oct. 2010.
[160] C. Chizhou, W. Peng, H. Wendong, M. Shijin, Z. Wenhuan, and Z. Yingwei, "Improved method for testing interphase insulation of drive motors in more electric aircraft under repetitive pulses," *High Voltage Eng.*, pp. 1–10, Apr. 2024.
[161] P. Wang et al., "Influence of ambient humidity on PDIV and endurance of inverter-fed motor insulation," in *2019 IEEE Elect. Insul. Conf.*, 2019, pp. 201–204.
[162] J. Harikumaran et al., "Failure modes and reliability oriented system design for aerospace power electronic converters," *IEEE Open J. Ind. Electron. Soc.*, vol. 2, pp. 53–64, Dec. 2020, doi: 10.1109/OJIES.2020.3047201.
[163] C. Liaw, P. Jhou, and C. Yang, "Switched-reluctance motor drive for more electric aircraft with energy storage buffer," *IEEE Trans. Aerosp. Electron. Syst.*, vol. 59, no. 6, pp. 7423–7439, Dec. 2023.
[164] M. Galea, P. Giangrande, V. Madonna, and G. Buticchi, "Reliability-oriented design of electrical machines: The design process for machines' insulation systems MUST evolve," *IEEE Ind. Electron. Mag.*, vol. 14, no. 1, pp. 20–28, Mar. 2020.
[165] G. Han, B. Chen, J. Hong, Z. Dong, and S. Xu, "Reliability evaluation method for power converters of speed synchronous dual-SRM drive," in *2023 26th Int. Conf. Elect. Mach. Syst.*, 2023, pp. 540–543.
[166] H. Chen, S. Xu, and S. Cui, "Reliability evaluation for power converter of SRM on fault-tolerance capability and thermal stress," *IEEE Trans. Ind. Electron.*, vol. 68, no. 2, pp. 1749–1758, Feb. 2021.
[167] H. Chen, F. Dong, S. Xu, J. Yang, and C. C. Chan, "Reliability evaluation of switched reluctance motor drive system in electric vehicle based on bayesian network," in *2019 IEEE Veh. Power Propulsion Conf.*, 2019, pp. 1–4.
[168] X. Chen, Z. Deng, and J. Peng, "Fault tolerant switched reluctance machine for fuel pump drive in aircraft," in *2009 4th IEEE Conf. Ind. Electron. Appl.*, 2009, pp. 2340–2344.
[169] X. Chen, Z. Deng, J. Peng, and X. Li, "Comparison of two different fault-tolerant switched reluctance machines for fuel pump drive in aircraft," in *2009 IEEE 6th Int. Power Electron. Motion Control Conf.*, 2009, pp. 2086–2090.
[170] H. Chen, G. Xie, and J. Jiang, "The two switched reluctance motors parallel drive system," in *Proc. Can. Conf. Elect. Comput. Eng.*, 2001, pp. 569–572.
[171] P. Peres, V. F. Pires, and J. F. Martins, "A novel spilt-winding fault-tolerant approach for a switched reluctance motor," in *Proc. IECON 2019-45th Annu. Conf. IEEE Ind. Electron. Soc.*, 2019, pp. 1538–1543.
[172] V. F. Pires, D. Foito, A. J. Pires, A. Cordeiro, and J. F. Martins, "A fault tolerant converter for a SRM drive based on a nine-switch inverter with a dual output," in *2023 IEEE 17th Int. Conf. Compat., Power Electron. Power Eng.*, 2023, pp. 1–6.
[173] C. Gan, X. Li, Z. Yu, K. Ni, S. Wang, and R. Qu, "Modular seven-leg switched reluctance motor drive with flexible winding configuration and fault-tolerant capability," *IEEE Trans. Transport. Electrific.*, vol. 9, no. 2, pp. 2711–2722, Jun. 2023.
[174] A. K. Rana and A. V. Ravi Teja, "A fault-tolerant power converter with multi-switch fault diagnosis and repair capability for 4-phase 8/6 SRM drives," *IEEE Trans. Transport. Electrific.*, vol. 8, no. 3, pp. 3896–3906, Sep. 2022.
[175] Q. Chen, D. Xu, L. Xu, J. Wang, Z. Lin, and X. Zhu, "Fault-tolerant operation of a novel dual-channel switched reluctance motor using two 3-phase standard inverters," *IEEE Trans. Appl. Supercond.*, vol. 28, no. 3, Apr. 2018, Art. no.5204205.
[176] V. F. Pires, D. Foito, A. J. Pires, A. Cordeiro, and J. F. Martins, "An 8/6 SRM drive with a multilevel converter based on an npc structure and designed to provide transistor fault tolerant capability," in *2022 IEEE 16th Int. Conf. Compatibility, Power Electron., Power Eng.*, 2022, pp. 1–6.
[177] V. F. Pires, A. Cordeiro, D. Foito, and A. J. Pires, "Multilevel converter with fault-tolerant capability for the switched reluctance machine," in *2021 28th Int. Workshop Electric Drives: Improving Rel. Electric Drives*, 2021, pp. 1–6.
[178] J. Borecki and B. Orlik, "Novel, multilevel converter topology for fault-tolerant operation of switched reluctance machines," in *2017 11th IEEE Int. Conf. Compat., Power Electron. Power Eng.*, 2017, pp. 375–380.
[179] T. G. Amaral, V. F. Pires, D. Foito, A. J. Pires, and J. F. Martins, "Fault detection and diagnosis technique for a SRM drive based on a multilevel converter using a machine learning approach," in *2023 12th Int. Conf. Renewable Energy Res. Appl.*, 2023, pp. 40–45.
[180] V. F. Pires, A. J. Pires, D. Foito, M. Chaves, and A. Cordeiro, "A fault tolerant multilevel converter topology for an 8/6 SRM drive based on a cross-switched configuration," in *2022 IEEE 8th Int. Conf. Energy Smart Syst.*, 2022, pp. 335–340.
[181] C. Yang, S. Song, C. Liu, J. Zhong, and G. Sun, "Development of high voltage switched reluctance starter/generator system for more electric aircarft," in *2023 IEEE 32nd Int. Symp. Ind. Electron.*, 2023, pp. 1–6.
[182] S. S. Yeoh, M. Rashed, M. Sanders, and S. Bozhko, "Variable-voltage bus concept for aircraft electrical power system," *IEEE Trans. Ind. Electron.*, vol. 66, no. 7, pp. 5634–5643, Jul. 2019.

Lefei Ge (Member, IEEE) was born in China, in 1992. He received the B.S. degree in measurement and control technology and the M.S. degree in electrical engineering from Northwestern Polytechnical University, Xi'an, China, in 2013 and 2016, respectively, and the Dr.-Ing. degree in electrical engineering from RWTH Aachen University, Aachen, Germany, in 2020.

In September 2016, he became a Research Associate with the Institute of Power Electronics and Electrical Drives, RWTH Aachen University. Since 2020, he has been an Associate Professor with the Department of Electrical Engineering, Northwestern Polytechnical University. His research interests include electrical machines and drives with emphasis on switched reluctance machines.

Nan Du (Student Member, IEEE) was born in China in 2001. She received the B.S. degree in electrical engineering and automation in 2023 from Northwestern Polytechnical University, Xi'an, China, where she is currently working toward the M.S. degree in electrical engineering.

Her research interests include motors and drives, with a focus on the control of permanent magnet synchronous motors and switched reluctance motors.

Jiahe Song was born in China, in 2001. She received the B.S. degree in electrical engineering in 2023 from Northeast Forestry University, Harbin, China, where she is currently working toward the M.S. degree in power energy.

Her research interests include electrical machines and drives with emphasis on the fault diagnosis of the switched reluctance machines.

Jiaxin Zhang was born in China, in 2001. He received the BS. degree in electrical engineering in 2023 from Northwestern Polytechnical University, Xi'an, China, where he is currently working toward the M.S. degree in power energy.

His research interests include various motors structures, control methods, and the topology design and drive design of switched reluctance motors.

Zizhen Fan was born in China, in 2000. She received the B.S. degree in electrical engineering in 2022 from Northwestern Polytechnical University, Xi'an, China, where she is currently working toward the M.S. degree in power energy.

Her research interests include electrical machines and drives with emphasis on the control of the permanent magnet synchronous motor drives and switched reluctance machines.

Dongpeng Zhang was born in China, in 2000. He received the B.S. degree in electrical engineering in 2022 from Northeast Forestry University, Harbin, China, where he is currently working toward the M.S. degree in power energy.

His current research focuses on position sensorless control algorithms for switched reluctance motors.

Shoujun Song (Senior Member, IEEE) received the B.S. and M.S. degrees in electrical engineering from Northwestern Polytechnical University, Xi'an, China, in 2003 and 2006, respectively, and the Dr.-Ing. degree in electrical engineering from the Technical University of Berlin, Berlin, Germany, in 2009.

He is currently a Professor with the Department of Electrical Engineering, Northwestern Polytechnical University. His research interests include electrical machines and drives with emphasis on switched reluctance machines and permanent magnet machines.